AD-A269 685

N-1862

June 1993

By T. Leslie Youd

Sponsored by
Office of Naval Technology

NCEL Technical Note

DTIC ELECTE SEP 22 1993 S E D

LIQUEFACTION-INDUCED LATERAL SPREAD DISPLACEMENT

Abstract Lateral ground displacements generated by liquefaction-induced lateral spread are a severe threat to the Navy's shore facilities. During past earthquakes, lateral spread displacements have pulled apart or sheared shallow and deep foundations of buildings, several pipelines and other structures and utilities that transect the ground displacement zone, buckle bridges or other structures constructed across the toe, and toppled retaining walls, bulkheads, etc. that lie in the path of the spreading ground. Port facilities have been particularly vulnerable to ground displacement because they are commonly sited on poorly consolidated natural deposits or fills that are particularly susceptible to liquefaction and lateral spread. This Technical Note presents methods for evaluating liquefaction susceptibility of sediments beneath level to gently sloping sites and for estimating magnitudes of potential lateral ground displacement at those sites. This design guide provides procedures including equations, tables, and charts required to evaluate liquefaction susceptibility beneath level and gently sloping sites and to estimate probable free-field lateral displacements at those sites. Free-field ground displacements are those that are not impeded by structural resistance, ground modification, or a natural boundary. This Technical Note does not provide guidance, however, for estimating ground settlements as a consequence of seismic compaction of granular soils or static consolidation of cohesive soils.

93 9 2 2

93-21910

NAVAL CIVIL ENGINEERING LABORATORY PORT HUENEME CALIFORNIA 93043-4328

Approved for public release; distribution unlimited

METRIC CONVERSION FACTORS

Approximate Conversions to Metric Measures

Symbol	When You Know	Multiply by	To Find	Symbol
		LENGTH		
in	inches	*2.5	centimeters	cm
ft	feet	30	centimeters	cm
yd	yards	0.9	meters	m
mi	miles	1.6	kilometers	km
		AREA		
in^2	square inches	6.5	square centimeters	cm^2
ft^2	square feet	0.09	square meters	m^2
yd^2	square yards	0.8	square meters	m^2
mi^2	square miles	2.6	square kilometers	km^2
	acres	0.4	hectares	ha
		MASS (weight)		
oz	ounces	28	grams	g
lb	pounds	0.45	kilograms	kg
	short tons (2,000 lb)	0.9	tonnes	t
		VOLUME		
tsp	teaspoons	5	milliliters	ml
Tbsp	tablespoons	15	milliliters	ml
fl oz	fluid ounces	30	milliliters	ml
c	cups	0.24	liters	l
pt	pints	0.47	liters	l
qt	quarts	0.95	liters	l
gal	gallons	3.8	liters	l
ft^3	cubic feet	0.03	cubic meters	m^3
yd^3	cubic yards	0.76	cubic meters	m^3
		TEMPERATURE (exact)		
°F	Fahrenheit temperature	5/9 (after subtracting 32)	Celsius temperature	°C

*1 in = 2.54 (exactly). For other exact conversions and more detailed tables, see NBS Misc. Publ. 286, Units of Weights and Measures, Price $2.25, SD Catalog No. C13.10:286.

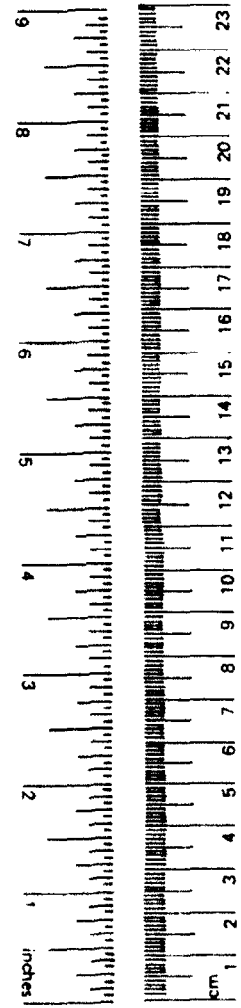

Approximate Conversions from Metric Measures

Symbol	When You Know	Multiply by	To Find	Symbol
		LENGTH		
mm	millimeters	0.04	inches	in
cm	centimeters	0.4	inches	in
m	meters	3.3	feet	ft
m	meters	1.1	yards	yd
km	kilometers	0.6	miles	mi
		AREA		
cm^2	square centimeters	0.16	square inches	in^2
m^2	square meters	1.2	square yards	yd^2
km^2	square kilometers	0.4	square miles	mi^2
ha	hectares (10,000 m^2)	2.5	acres	
		MASS (weight)		
g	grams	0.035	ounces	oz
kg	kilograms	2.2	pounds	lb
t	tonnes (1,000 kg)	1.1	short tons	
		VOLUME		
ml	milliliters	0.03	fluid ounces	fl oz
l	liters	2.1	pints	pt
l	liters	1.06	quarts	qt
l	liters	0.26	gallons	gal
m^3	cubic meters	35	cubic feet	ft^3
m^3	cubic meters	1.3	cubic yards	yd^3
		TEMPERATURE (exact)		
°C	Celsius temperature	9/5 (then add 32)	Fahrenheit temperature	°F

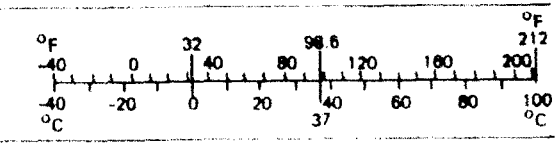

REPORT DOCUMENTATION PAGE

Form Approved
OMB No. 0704-0188

Public reporting burden for this collection of information is estimated to average 1 hour per response, including the time for reviewing instructions, searching existing data sources, gathering and maintaining the data needed, and completing and reviewing the collection of information. Send comments regarding this burden estimate or any other aspect of this collection of information including suggestions for reducing this burden, to Washington Headquarters Services, Directorate for Information Operations and Reports, 1215 Jefferson Davis Highway, Suite 1204, Arlington, VA 22202-4302, and to the Office of Management and Budget, Paperwork Reduction Project (0704-0188), Washington, DC 20503.

1. AGENCY USE ONLY (Leave blank)	2. REPORT DATE	3. REPORT TYPE AND DATES COVERED
	June 1993	Final: Oct 1992 - Oct 1993

4. TITLE AND SUBTITLE

LIQUEFACTION-INDUCED LATERAL SPREAD DISPLACEMENT

5. FUNDING NUMBERS

PR - RM33F60-001-0106
WU - DN387338

6. AUTHOR(S)

T. Leslie Youd

7. PERFORMING ORGANIZATION NAME(S) AND ADDRESS(ES)

Brigham Young University
Provo, Utah 84602

8. PERFORMING ORGANIZATION REPORT NUMBER

TN-1862

9. SPONSORING/MONITORING AGENCY NAME(S) AND ADDRESS(ES)

Office of Naval Technology
Arlington, VA 22217-5000

10. SPONSORING/MONITORING AGENCY REPORT NUMBER

11. SUPPLEMENTARY NOTES

12a. DISTRIBUTION/AVAILABILITY STATEMENT

Approved for public release; distribution unlimited.

12b. DISTRIBUTION CODE

13. ABSTRACT (Maximum 200 words)

Lateral ground displacements generated by liquefaction-induced lateral spread are a severe threat to the Navy's shore facilities. During past earthquakes, lateral spread displacements have pulled apart or sheared shallow and deep foundations of buildings, several pipelines and other structures and utilities that transect the ground displacement zone, buckle bridges or other structures constructed across the toe, and toppled retaining walls, bulkheads, etc. that lie in the path of the spreading ground. Port facilities have been particularly vulnerable to ground displacement because they are commonly sited on poorly consolidated natural deposits or fills that are particularly susceptible to liquefaction and lateral spread. This Technical Note presents methods for evaluating liquefaction susceptibility of sediments beneath level to gently sloping sites and for estimating magnitudes of potential lateral ground displacement at those sites. This design guide provides procedures including equations, tables, and charts required to evaluate liquefaction susceptibility beneath level and gently sloping sites and to estimate probable free-field lateral displacements at those sites. Free-field ground displacements are those that are not impeded by structural resistance, ground modification, or a natural boundary. This Technical Note does not provide guidance, however, for estimating ground settlements as a consequence of seismic compaction of granular soils or static consolidation of cohesive soils.

14. SUBJECT TERMS

Ground deformation, lateral spreading, liquefaction

15. NUMBER OF PAGES

57

16. PRICE CODE

17. SECURITY CLASSIFICATION OF REPORT	18. SECURITY CLASSIFICATION OF THIS PAGE	19. SECURITY CLASSIFICATION OF THIS PAGE	20. LIMITATION OF ABSTRACT
Unclassified	Unclassified	Unclassified	UL

CONTENTS

ABSTRACT ii

Section 1. INTRODUCTION 1

1.1. SCOPE 1

1.2. APPLICATION 1

1.3. REFERENCE 1

Section 2. LIQUEFACTION SUSCEPTIBILITY 1

2.1. EVALUATION PROCEDURES 1

2.2. SIMPLIFIED EMPIRICAL PROCEDURE 2

2.3. EXAMPLE CALCULATION 6

Section 3. LATERAL DISPLACEMENT 8

3.1. MODES OF FAILURE 8

Section 4. ANALYSIS OF LATERAL DISPLACEMENT 10

4.1. METHOD OF ANALYSIS 10

4.2. DEVELOPMENT OF EMPIRICAL EQUATIONS 11

4.3. APPLICATION OF EQUATIONS 15

4.4. EXAMPLE CALCULATIONS 20

Section 5. REFERENCES 22

Accesion For
NTIS CRA&I ☒
DTIC TAB ☐
Unannounced ☐
Justification
By
Distribution /
Availability Codes
Dist | Avail and / or Special
A-1

DTIC QUALITY INSPECTED 1

Section 1. INTRODUCTION

1.1. SCOPE.

Methods are presented herein for evaluating liquefaction susceptibility beneath level to gently sloping sites and for estimating potential lateral ground displacement at those sites (for slopes with gradients less than 6%) This guideline does not consider ground settlement as a consequence of seismic compaction of granular soils or static consolidation of cohesive soils.

1.2. APPLICATION.

Liquefaction of saturated granular soils and consequent ground deformation have been a major cause of damage to constructed works during past earthquakes. Loss of bearing strength, differential settlement, and horizontal displacement due to lateral spread are the major types of ground deformation beneath level to gently sloping sites. This design guide provides procedures including equations, tables, and charts required to evaluate liquefaction susceptibility beneath level or gently sloping sites and to estimate probable free-field lateral displacements at those sites. Free-field ground displacements are those that are not impeded by structural resistance, ground modification or a natural boundary.

These procedures may be used for assessment of liquefaction-induced lateral ground displacements. The results may be used for preliminary assessment of ground-failure hazard to constructed or planned facilities, for initial lateral displacement design criteria (although structural impedance may prevent development of full free-field displacements), and for delineation of areas where liquefaction-induced earthquake damage might be expected.

1.3. REFERENCE

Bartlett, S.F., and Youd, T.L., 1992, Empirical analysis of horizontal ground displacement generated by liquefaction-induced lateral spread: National Center for Earthquake Engineering Research, Technical Report NCEER-92-0021.

LIQUEFACTION SUSCEPTIBILITY

2.1. EVALUATION PROCEDURES.

The following evaluation procedure is based on commentary to the NEHRP Recommended Provisions for the Development of Seismic Regulations for New Buildings (BSSC, 1991). Liquefaction susceptibility at a site is commonly expressed in terms of a factor of safety against the occurrence of liquefaction. This factor is defined as the ratio between available soil resistance to liquefaction, expressed in terms of the cyclic stresses required to cause soil liquefaction, and the cyclic stresses generated by the design earthquake. Both of these parameters are commonly normalized with respect to the effective overburden stress at the depth in question.

The following possible methods for calculating the factor of safety against liquefaction have been proposed and used to various extents:

2.1.1. Analytical Methods.

These methods typically rely on laboratory test results to determine either liquefaction resistance or soil properties that can be used to predict the development of liquefaction. Various equivalent linear and nonlinear computer methods are used with the laboratory data to evaluate the potential for liquefaction. Because of the considerable difficulty in obtaining undisturbed samples of loose granular (liquefiable) sediment for laboratory evaluation of constitutive soil properties, the use of analytical methods, which rely on accurate measurements of constitutive properties, are usually limited to critical projects or to research.

2.1.2. Physical Modeling.

These methods typically involve the use of centrifuges or shaking tables to simulate seismic loading under well-defined boundary conditions. Soil used in the model is reconstituted to represent different density and geometrical conditions. Because of difficulties in precisely modeling of insitu conditions at natural sites, physical models are seldom used in design studies for specific sites. Physical models are valuable, however, for analyzing and understanding generalized soil behavior and for evaluating the validity of constitutive models under well-defined boundary conditions.

2.1.3. Empirical Procedures.

Because of difficulties in analytically or physically modeling soil conditions at liquefiable sites, the use of empirical methods has become a standard procedure in routine engineering practice. Procedures for carrying out a liquefaction assessment using the empirical method are summarized below. More detail on development of the methods is given by the National Research Council (NRC, 1985).

2.2. SIMPLIFIED EMPIRICAL PROCEDURE.

For most empirical analyses, the average earthquake-induced cyclic shear stress is estimated either from the simple equation listed below (Equation 1) or from dynamic response analyses using computer codes such as SHAKE, DESRA, etc. Application of the simple equation yields a factor called the "cyclic stress ratio" generated by the earthquake (CSRE) which is commonly written as τ_{av}/σ'_o, where τ_{av} is the average earthquake-induced cyclic shear stress and σ'_o is the pre-earthquake effective overburden stress.

$$\text{CSRE} = \tau_{av}/\sigma'_o = 0.65\ (a_{max}/g)(\sigma_o/\sigma'_o)r_d \qquad (1)$$

Other factors in the equation are the peak horizontal acceleration at ground surface expressed as a decimal fraction of gravity, (a_{max}/g), the vertical total stress in the soil at the depth in question, σ_o, and a depth-related stress reduction factor, r_d. The chart reproduced in Figure 1 is used to estimate r_d. In standard practice, a_{max} is the peak horizontal ground acceleration that would have occurred at the site in the absence of a rise of pore-water pressure.

To determine liquefaction resistance of sandy soils, the cyclic stress ratio computed from Equation 1 is compared to the cyclic stress ratio required to generate liquefaction (CSRL) at the site in question for the given design earthquake. The factor of safety against liquefaction is then written as:

$$FS = CSRL/CSRE \qquad (2)$$

The most common technique for estimating CSRL is from an empirical relationship between cyclic stress ratio and normalized blow count, $(N_1)_{60}$. That relationship is depicted by empirical curves plotted by Seed and others (1985), which divides sites that liquefied historically from those that did not on the basis of $(N_1)_{60}$. Figure 2 shows that relationship for magnitude 7.5 earthquakes and soils with varying percentages of fines. The points on the figure are cyclic stress ratios calculated from tested field sites. Solid dots represent sites where liquefaction occurred and open dots represent sites where surface evidence of liquefaction was not found. The curves were drawn through the data to separate regions where liquefaction did and did not develop. Although the curves drawn by Seed and others (1985) envelope the plotted data, it is possible that liquefaction may have occurred beyond the enveloped data, but was not detected at ground surface. Consequently, a factor of safety of 1.2 is appropriate in engineering design. The factor to be used is based on engineering judgement with appropriate consideration given to type and importance of structure and the potential for ground deformation.

The maximum acceleration, a_{max}, commonly used in liquefaction analysis is the peak horizontal acceleration that would occur at the site in the absence of liquefaction. Thus, the a_{max} used in Equation 1 is the estimated rock-outcrop acceleration corrected for local soil response, but without consideration of excess pore-water pressures that might develop.

Methods commonly used to estimate a_{max} include: a) estimates from standard peak acceleration attenuation curves valid for comparable soil conditions; b) estimates from standard peak acceleration attenuation curves for bedrock sites, with correction of a_{max} for local site effects using standard site amplification curves, such as those given by Seed et al., (in press) [Figure 13, herein] or, more preferably, using computerized site response analysis; and c) from probabilistic maps of a_{max}, with or without correction for site amplification or attenuation depending on the rock or soil conditions used to generate the map.

Because Figure 2 is only applicable to magnitude 7.5 earthquakes, a magnitude scaling factor is required to correct the results from Figure 2 to other magnitudes of earthquakes. The most commonly used magnitude scaling factors are listed in Table 1 (NRC, 1985). The magnitude, M, required to determine a magnitude scaling factor from Table 1 should correspond to the design earthquake selected for the liquefaction evaluation. Preferably moment magnitude, M_w, should be used in the liquefaction analyses, but for magnitudes less than 7.5, either M_s or M_L may be used. If alternative c) is selected, the definition of M is not obvious and additional studies and considerations are necessary. In this instance, an engineering seismologist should be consulted to select an appropriate magnitude. In all instances, it should be remembered that the likelihood of liquefaction at the site is a function of both a_{max} and M. Because of the longer duration of strong ground shaking, large distant earthquakes may generate liquefaction at a site while smaller nearby earthquakes may not even though the a_{max} generated by the distant events is smaller than that generated by the nearby shocks.

To adjust CSRL for earthquake magnitudes larger or smaller than 7.5, the cyclic stress ratio determined from Figure 2 is corrected by a magnitude scaling factor taken from Table 1. As the

magnitude increases, that scaling factor decreases. For example, for an $(N_1)_{60}$ of 20, a clean sand (fines content < 5%) and an earthquake magnitude of 7.5, the CSRL determined from Figure 2 is 0.22. For the same site conditions, but for an earthquake magnitude of 8.0, the determined ratio of 0.22 is multiplied by a magnitude scaling factor of 0.89 (interpolated from Table 1) to yield a CSRL of 0.20. Similarly, for an earthquake magnitude of magnitude 6.0, the magnitude scaling factor is 1.32 and the CSRL is 0.29. Thus, a magnitude 6.5 earthquake would have to generate a CSRE of 0.29 to reach the threshold for liquefaction, whereas, a magnitude 7.5 earthquake would reach the threshold at a CSRE of 0.22 and a magnitude 8 event would reach the threshold at a CSRE of 0.20.

Seed and Harder (1990) suggest correcting CSRL for two additional factors, k_σ and k_α which are used to correct CSRL for the influence of soil depth and the presence of static shear stress (from a sloping ground condition), respectively. k_σ corrects CSRL for the effects large effective overburden pressures; that is, as effective overburden pressure increases, the cyclic stress ratio required to cause liquefaction (CSRL) effectively decreases. For liquefiable materials at shallow depths, say less than 40 ft where most lateral spreads occur, the k_σ-correction factor is generally near 1.0. Also, because sediments generally become more resistant to liquefaction with age and because the age of natural deposits generally increase with depth, the effects of overburden pressure are counterbalanced to large degree by the influence of age. Thus, because the influence of the k_σ-factor is not great at shallow depths and because natural sediments generally increase in liquefaction resistance with depth due to aging, no correction for effective overburden pressure is suggested for estimation of liquefaction susceptibility at shallow depths (less than 40 ft) at natural sites.

Similarly, the value of k_α is near 1.0 for small static driving shear stresses. Lateral spreads generally occur on gently sloping ground (slopes of less than 6 percent), where driving shear stresses are sufficiently small that the k_α-correction can be safely neglected.

The corrected blow count, $(N_1)_{60}$, required for evaluation of soil liquefaction resistance is commonly determined from measured standard penetration resistance, N_m but may also be determined from cone penetration (CPT) resistance using standard correlations to estimate N_m values from the CPT data. $(N_1)_{60}$ is calculated from N_m as follows:

$$(N_1)_{60} = C_n\,(ER_m/60)\,N_m \qquad (3)$$

where C_n is a factor that corrects N_m to an effective overburden pressure of 1 tsf, and ER_m is the measured hammer energy ratio which is defined as the percent of theoretical free-fall hammer energy that is actually transferred to the drill rod during hammer impact. The curve plotted in Figure 3 is typically used to evaluate C_n. As an alternative, Liao and Whitman (NRC, 1985) suggests that the following equation can be used to estimate C_n.

$$C_n = (1/\sigma_v')^{1/2} \qquad (4)$$

where σ_v' is expressed in tons per square foot.

Measured hammer energy ratios or estimates of ratios from tabulations such as in Table 2 are used to define ER_m. An additional correction should be made to $(N_1)_{60}$ for shallow soil layers where the length of drilling rod is 10 ft or less. In those instances, $(N_1)_{60}$ should be multiplied by a factor of 0.75 to correct for poor hammer-energy transfer associated with short rod lengths (Seed et al., 1985).

Because the variety of equipment and procedures used to conduct standard penetration tests, and because the measured blow count, N_m, is sensitive to equipment and operational procedures, the following commentary and guidance is given with respect to the SPT test. Special attention must be given to the determination of normalized blow count, $(N_1)_{60}$, used in Figure 3. When developing the empirical relation between blow count and liquefaction resistance, Seed and his colleagues recognized that the blow count from the SPT is greatly influenced by factors such as the method of drilling, the type of hammer, the sampler design, and type of mechanism for lifting and dropping the hammer, etc. The magnitude of these variations are shown by the data in Table 2. In order to reduce variability in the measurement of N, Seed and his colleagues (Seed and others, 1983; 1985) suggest the following procedures and specifications for SPT tests for liquefaction investigations.

- The impact should be delivered by a rope and drum system with two turns of the a rope around the rotating drum to lift a hammer weighing 140 lb, or more preferably a drive system should be used for which ER_m has been measured or can be reliably estimated.

- The hole should be approximately 4 in (100 mm) diameter and drilled with a tricone or baffled drag bit that produces upward deflection of the drilling fluid to prevent erosion or disturbance to the soil below the cutting edge of the bit. Bentonitic drilling mud should be used for borehole stability, and special care is required to assure that the drilling fluid level in the hole never drops below the ground water table.

- A or AW rod should be used in holes less than 50 ft deep. N or NW rod should be used in deeper holes.

- The split spoon sampling tube should be equipped with liners or otherwise have a constant internal diameter of 1 3/8 in.

- Application of blows should be at a rate of 30 to 40 blows per minute. (Some engineers suggest that a slower rate of 20 to 30 blows per minute is easier to achieve and control and gives comparable results.) The blow count, N_m, is determined by counting the blows required to drive the penetrometer through the depth interval of 1 ft, from 6 in to 18 in below the bottom of the hole.

FAILURE TO FOLLOW THESE STANDARD GUIDELINES, AS UNFORTUNATELY ALL TO COMMONLY OCCURS IN PRACTICE, INTRODUCES LARGE UNCERTAINTIES INTO LIQUEFACTION ASSESSMENTS.

Use of the cone penetration test (CPT) to measure penetration resistance and estimate N has the advantage that the CPT yields a continuous record of penetration and frictional resistance with depth. The primary disadvantage of the cone test is that soil samples are not retrieved during CPT sounding. Thus, this test should be used in conjunction with other drilling and sampling. The preferable sequence would be to conduct CPT soundings to delineate subsurface stratigraphy and estimate soil properties. Based on that information, further field testing and sampling, including SPT tests, could then be optimally planned. Laboratory tests should be conducted on samples for soil classification and for determination of mean grain size, D_{50}, and fines content, F. Several correlations have been prepared for estimating N from cone penetration resistance, including the summary plot by Kulhawy and Mayne shown in Figure 4. From these correlations, reasonable estimates of N can be determined from cone penetration resistance, q_c, and D_{50}.

For liquefaction analyses, the curve by Robertson and Campanella (shown on Figure 4) should be used because (1) it gives reasonably conservative estimates of N (approximately mean plus one standard deviation for the total data set) and 2) that correlation has been more widely used in the past for liquefaction evaluations, and thus has a stronger empirical base for estimating liquefaction hazard. As a final note, only standard electrical CPT devices should be used for liquefaction investigations: mechanical CPT devices may give disparate records for tests in liquefiable soils.

Soils composed of sands, silts, and gravels are most susceptible to liquefaction while clayey soils are generally immune to this phenomenon. The curves in Figure 2 are valid for soils composed primarily of sand. The curves should be used with caution for soils with substantial amounts of gravel. Verified corrections for gravel content have not been developed; a geotechnical engineer, experienced in liquefaction hazard evaluation, should be consulted when gravelly soils are encountered. For soils containing more than 35% fines, the curve for 35% fines Figure 2) should be used as a conservative estimate, provided the following criteria suggested by Seed and others (1983) are met:

- The weight of soil particles finer than 0.005 mm (clay-size particles) is less than 15% of the dry weight of a specimen of the soil.
- The liquid limit of soil is less than 35%.
- The moisture content of the in-place soil is greater than 0.9 times the liquid limit.

2.3. EXAMPLE CALCULATION.

The empirical procedure for calculation of factor of safety against liquefaction is illustrated through the following example calculations.

(1) The first step in a calculation of liquefaction susceptibility is to determine the design peak horizontal acceleration, a_{max}, and earthquake magnitude, M. Procedures for making these estimates are given in other guides, such as TM 5-8-9-10-1/NAVFACP-355.1/AFM88-3, Chapter 13, Section A (Specification of Ground Motion). For this example, we shall assume a design earthquake with a magnitude of 6.5 that produces a peak acceleration of 0.30 g at the site in question.

(2) The second step is to develop a characteristic soil profile for the locality to be evaluated. Procedures such as those outlined in NAVFAC DM-7.1 Chapters 2 (Field Exploration, Testing and Instrumentation) and 3 (Laboratory Testing) should be used to delineate and define soil stratigraphy. These manuals also provide suggested procedures for drilling and retrieving samples, and for conducting of classification and index tests. For this example calculation, we shall assume the soil profile shown on Figure 5 and the soil properties listed in Table 3 are representative of the site.

(3) The third step is to calculate the cyclic stress ratio generated by the earthquake (CSRE) at each depth in question. For example, CSRE might be calculated at the depth of each standard penetration test or it might be calculated and plotted as a continuous curve versus depth. Several computer programs are available that facilitate these calculations. For this example, however, we will follow a step by step procedure to illustrate the calculation of CSRE at a depth of 15 ft. From Equation 1,

$$CSRE = \tau_{av}/\sigma'_o = 0.65\ (a_{max}/g)(\sigma_o/\sigma'_o)r_d \qquad (1)$$

The total overburden pressure, σ_v, at a depth of 15 ft for this example is:

$$\sigma_v = (110\ lb/ft^3)(5.0\ ft) + (120\ lb/ft^3)(10.5\ ft) = 1{,}750\ lb/ft^2$$

The effective overburden pressure, σ'_v, for this example is:

$$\sigma'_v = \sigma_v - u = 1{,}750\ lb/ft^2 - (15\ ft - 4\ ft)(62.4\ lb/ft^3) = 1{,}064\ lb/ft^2$$

where u is pore-water pressure. From Figure 1, the coefficient r_d at a depth of 15 ft is 0.97. Applying these values in equation 1 yields the following CSRE:

$$CSRE = \tau_{av}/\sigma'_o = (0.65)(0.30\ g)(1{,}750\ lb/ft^2/1{,}064\ lb/ft^2)(0.97) = 0.31$$

(4) The fourth step is to calculate the cyclic stress ratio required to cause liquefaction (CSRL). That ratio is determined by correlation with $(N_1)_{60}$ through the curves drawn on Figure 2.

$$(N_1)_{60} = C_n\ (ER/60)\ N_m \qquad (3)$$

For this example, we assume an energy ratio for the standard penetration hammer used in the field SPT test was measured at 50%. C_n may be determined directly from Figure 3. For an effective overburden pressure of 1,064 lb/ft^2 (1.06 Kip/ft^2), $C_n = 1.37$. Thus,

$$(N_1)_{60} = (1.37)(50/60)(12\ blows/ft) = 13.6\ blows/ft$$

This value along with all the other calculated $(N_1)_{60}$ values for this example soil profile are listed in Table 3 and plotted on Figure 5.

From the curves in Figure 2, an $(N_1)_{60}$ of 13.6 yields a CSRL of 0.17, which is the minimum CSRL that is required to generate liquefaction for a magnitude 7.5 earthquake. To correct the CSRL to a magnitude 6.5 earthquake, the CSRL of 0.17 must be multiplied by the appropriate magnitude scaling factor interpolated from Table 1. For a magnitude 6.5 earthquake, that factor is 1.19. Thus, the minimal CSRL required to cause liquefaction at a 15-ft depth in the given soil profile is:

$$CSRL = (1.19)(.17) = 0.20$$

(5) The factor of safety against liquefaction at a depth of 15 ft in the soil profile is calculated from Equation 2:

$$FS = CSRL/CSRE = 0.20/0.31 = 0.65$$

Thus, liquefaction would be expected to readily develop at a depth of 15 ft for the given design earthquake and site conditions. Factors of safety calculated for the depth of each standard penetration test in the soil profile are listed in Table 3 and plotted on Figure 5.

(6) As noted above, for soils containing more than 35% fines the curves in Figure 2 may be used as a conservative estimate for liquefaction hazard, provided that all of the following criteria suggested by Seed and others (1983) are met:

- The weight of soil particles finer than 0.005 mm (clay-size particles) is less than 15% of the dry weight of a specimen of the soil.
- The liquid limit of soil is less than 35%.
- The moisture content of the in-place soil is greater than 0.9 times the liquid limit.

For example, consider the soil in the silty clay layer at a depth of 21 ft to 24 ft as shown on Figure 5. The silt in that layer has a clay content of 13%, a liquid limit of 31% and a plastic limit of 22%, and a natural moisture content of 26%.

- By criterion 1, the soil clay content of 13% is less than 15%, which does not exclude liquefaction.
- By criterion 2, the liquid limit of 32% is less than 35%, which does not exclude liquefaction.
- By criterion 3, the moisture content of the soil of 26% is less than 0.9 times the liquid limit of 32% (i.e. 0.9 X 32% = 29% >26%), which excludes liquefaction because the silt is over consolidated and thus immune to liquefaction.

Because the sediment in question does not meet all three of the criteria, the layer is classed as non-liquefiable.

Section 3 LATERAL DISPLACEMENT

3.1. MODES OF FAILURE.

Liquefaction may lead to any one of three types of ground failure that produce lateral ground displacement--flow failure, lateral spread and ground oscillation. The bounds between these failure types are transitional and which type of failure that develops, if any, depends on local site conditions.

Flow failures form on steep slopes (greater than 6%), are caused by a large reduction of soil strength (contractive soils), and are characterized by large displacements (tens of feet or more) with substantial internal disruption of the mobilized soil mass (as depicted in Figure 6). Figure 7 shows a flow failure that developed in a highway fill at the western edge of Lake Merced in San Francisco during the 1957 Daly City earthquake.

On the other end of the spectrum, **ground oscillation** generally occurs on flat ground with liquefaction at depth decoupling surface soil layers from the underlying unliquefied ground (Figure 8). This decoupling allows rather large transient ground oscillations or ground waves to develop; the associated permanent displacements, however, are usually small and chaotic with respect to magnitude and direction. Observers of ground oscillation have described large-amplitude ground waves (up to several

feet high) often accompanied by opening and closing of ground fissures, which in some instances have propelled ejected ground water to heights as great as tens of feet. For example, most of the chaotic ground movements which fractured and buckled pavements in the Marina District of San Francisco during the 1989 Loma Prieta earthquake were caused by ground oscillation.

Lateral spread lies between flow failure and ground oscillation on the ground failure spectrum and involves some components of both of these end members. Lateral spread is characterized primarily by horizontal displacement of surficial soil layers as a consequence of liquefaction of a subsurface granular deposit (Figure 9). Displacement occurs in response to a combination of dynamic earthquake-generated inertial forces and static gravitational forces acting on soil layers within and above the liquefied zone. During failure, the surface layers commonly break into large blocks which transiently shift back and forth and up and down in the form of ground waves (ground oscillation) but move progressively down slope. Lateral spreads generally move down gentle slopes (usually less than 6%) or slip toward a free face such as an incised river channel. Horizontal displacements may range from a few inches to a few feet, but where ground conditions are particularly favorable or shaking is very intense or of long duration, displacements may be larger and may even approach a flow-failure condition. Figure 10 shows the Marine Sciences Laboratory at Moss Landing, California that was pulled apart by a lateral spread that migrated about 5 ft down a mild slope during the 1989 Loma Prieta earthquake. A lateral spread with larger horizontal displacement (about 12 ft) developed at that same site during the 1906 San Francisco earthquake.

The surface of a lateral spread is commonly disrupted by open fissures and scarps at the head of the failure, shear zones along the margins, and compressed or buckled soil at the toe. Ground fissures and small grabens also may develop within the interior of the mass. Differential vertical displacements may also occur as a consequence of down-slope movement, compaction of underlying granular sediment, or dynamic penetration or rise of discrete soil blocks. Lateral spreads commonly pull apart or shear foundations of buildings and other structures built on or across the head of the failure zone, sever pipelines and other structures and utilities that transect the lateral margins of the zone, and topple retaining walls or buckle pipelines, bridges or other structures constructed across the toe. For example, port facilities are commonly sited on poorly consolidated natural deposits or fill that is susceptible to liquefaction and lateral spread. Spreads at these facilities have distorted structures, disrupted pavements, bowed crane rails, toppled or tilted quay walls, etc.

This design guide develops procedures for predicting displacement of lateral spreads rather than flow failure or ground oscillation for the following reasons. (1) The range of displacements associated with lateral spread (commonly up to a several feet) are more applicable to the design and protection of common engineered construction. For displacements of this magnitude, structural measures might be applied to strengthen construction to reduce damage. (2) Flow failure displacements are usually exceed tens of feet or larger and are so destructive that estimation of displacement is of secondary importance. For flows, the primary question is usually whether liquefaction will occur and trigger a failure. Dynamic stability analyses, such as those used for earth dams, may be applicable for engineering hazard evaluations for such sites. In those analyses, undrained steady-state or residual strength is usually the key soil parameter for assessing stability. Further guidance on those analyses is beyond the scope of this guideline. (3) Very little study has been made of displacements associated with ground oscillation. Thus, standard techniques for estimating displacements, either transient or permanent, are not available. Analytical techniques (such as finite element and sliding block analyses described below) might be useful for estimating displacements, if the appropriate values for soil properties can be determined.

Section 4. ANALYSIS OF LATERAL DISPLACEMENT

4.1. METHOD OF ANALYSIS.

Several techniques have been proposed for estimating lateral ground displacements at liquefaction sites, including analytical models, physical models and empirical correlations:

4.1.1. Finite Element Analyses.

Two non-linear finite element analyses have been proposed for evaluation of ground deformation at liquefaction sites--the Princeton University effective stress model (Prevost, et al., 1986) and TARA-3FL (Finn and Yogendrakumar, 1989). These analyses require constitutive stress-strain relationships and undrained steady state strength data, respectively. Because of inherent difficulties in sampling and testing to define these properties for field sites, applications of these procedures are usually limited to critical projects or to research.

4.1.2. Sliding-Block Analyses

Newmark (1965) introduced a rather simple mechanistic procedure for estimating the displacement of a rigid block resting on an inclined failure plane that is subjected to earthquake shaking. That model can be analyzed as a single-degree-of-freedom rigid plastic system. As Byrne et al. (1992) have noted, there are two concerns when applying Newmark's simple model to a natural ground failures, such as lateral spreads: (1) the soil, particularly in liquefiable zones, is not adequately modeled as a rigid-plastic material; and (2) the single-degree-of-freedom model does not allow for a pattern of displacements to be computed. The latter deficiency is critical to lateral spreads near free faces, where displacements markedly decrease with distance from the free face. For this type of failure, a single-degree-of-freedom model is incapable of generating such a distribution of displacements. To overcome these obstacles, Byrne et al. (1992) have developed a more sophisticated model in which a deformational analysis incorporating pseudo-dynamic finite element procedures that allow consideration of both the inertia forces from the earthquake as well as softening of the liquefied soil. The method is essentially an extension of Newmark's simple model to a flexible multi-degree-of-freedom system.

Application of the procedure by Byrne et al. (1992) requires evaluation of several model-specific soil properties, and application of rather sophisticated computer programs, such as SOILSTRESS, which are proprietary. The mechanistic technique is still being developed and has not progressed to the point where the method is available for routine engineering analyses. For analysis of critical structures, specialists may be available to apply the procedure. This mechanistic technique, however, has the advantage of most mechanical models, in that the influence of various soil conditions and possible remedial measures can be modeled and analyzed.

4.1.3. Physical Modeling

Physical modeling typically involves use of centrifuges or shaking tables to simulate seismic loading under well-defined boundary conditions. The soil used in such models is reconstituted to represent different density and geometrical conditions. Because of difficulties in precisely modeling field conditions

at liquefiable sites, physical models have seldom been used in design studies for specific sites. Physical models are valuable, however, for analyzing and understanding generalized soil behavior and for evaluating the validity of constitutive models under well-defined boundary conditions.

4.1.4. Empirical Procedures

Because of the present difficulties in analytically or physically modeling soil conditions at liquefiable sites, empirical methods have become a standard procedure for determining liquefaction susceptibility and are now available for estimating lateral spread displacement. Recommended procedures for estimating displacements are given below. These empirical procedures have the advantage of using standard field tests and soil classification properties for estimating lateral displacement. More details on the development of the procedures are given by Bartlett and Youd (1992).

For general engineering applications, where a high degree of accuracy is not required, empirical analysis are adequate and can be conservatively applied for basic engineering design. Where more accuracy is required, the empirical estimates may be improved by the more sophisticated finite element or mechanistic sliding-block analyses. For these more sophisticated analyses, more refined soil property data are required, such as constitutive stress-strain relations and steady state undrained or residual strengths. Because of the difficulty in precisely determining these more refined soil properties at field sites, estimates from the more sophisticated procedures may be no more accurate than empirical estimates. Thus, this guide emphasizes the empirical approach.

4.2. DEVELOPMENT OF EMPIRICAL EQUATIONS.

Bartlett and Youd (1992) collected lateral spread case history data from eight earthquakes and numerous lateral spreads. The earthquakes and principle localities of spreading are listed in Table 4. Six of the earthquakes are from the western U.S. and the other two are from Japan. The lateral spread data from the Japanese earthquakes are from a narrow range of seismic conditions, magnitude 7.5 and 7.7 earthquakes at source distances of 21 to 30 km. The six U.S. earthquakes span a wider range of magnitudes (6.4 to 9.2) and greater range of source distances (up to 90 km), but all come from the western U.S., which is characterized by relatively high ground motion attenuation with distance from the seismic source. Also, most of the lateral spread areas are underlain by stiff soils (mostly deep profiles of cohesionless sands and/or overconsolidated silts and clays). Thus, the observational data are primarily from stiff sites in regions of relatively high ground motion attenuation.

From published case-histories of lateral spreads, Bartlett and Youd compiled a database of 448 horizontal displacement vectors and 270 associated nearby bore-hole logs. To increase the database for distant sites, they added information for 19 sites near the maximum distance bound for observed liquefaction effects (Ambraseys, 1988, Table VII). Those distant sites are primarily from the western U.S. Effects at those distant sites typically consisted of a few small sand boils and, in some instances, a few small fissures. Lateral displacement and soil-property information were not reported for those distant sites. To provide reasonable estimates for the regression analysis, Bartlett and Youd assigned uniform displacements of 0.05 m to each of the distant sites, and uniform soil profiles consisting of the average thicknesses and soil properties of sediments beneath the lateral spreads in the database. From these compiled data, Bartlett and Youd applied the technique of stepwise multiple linear regression (MLR) to

first define the factors that most influence ground displacement, and then to construct a regression model incorporating those factors.

Several possible seismic, geometric, and soil factors were considered in the regression analyses. Although seismic factors, such as peak acceleration, a_{max}, and duration of strong shaking, t_{ss}, should be fundamental parameters controlling displacement, the regression yielded better results (higher correlation coefficients) when magnitude, M, and horizontal distance from the seismic source, R, were used as seismic parameters. One reason M and R performed better is that those parameters could be directly measured, whereas a lack of instrumental records at lateral spread sites necessitated the estimation of a_{max} and t_{ss} from M and R. Therefore, the regression model is in expressed in terms of M and R.

To incorporate the influence of geometric factors, two statistically independent models are required--a free-face model for areas near steep banks, and a ground-slope model for areas with gently sloping terrain. Several soil factors were tested in the models; those that were statistically significant are incorporated into the following equations:

For free-face conditions:

$$\text{LOG } D_H = -16.3658 + 1.1782\,M - 0.9275\,\text{LOG } R - 0.0133\,R + 0.6572\,\text{LOG } W + 0.3483\,\text{LOG } T_{15} + 4.5270\,\text{LOG } (100 - F_{15}) - 0.9224\,D50_{15} \quad (5)$$

For ground slope conditions:

$$\text{LOG } D_H = -15.7870 + 1.1782\,M - 0.9275\,\text{LOG } R - 0.0133\,R + 0.4293\,\text{LOG } S + 0.3483\,\text{LOG } T_{15} + 4.5270\,\text{LOG } (100 - F_{15}) - 0.9224\,D50_{15} \quad (5b)$$

Where:

D_H = Estimated lateral ground displacement in meters (multiply by 3.3 to convert to feet)

$D50_{15}$ = Average mean grain size in granular layers included in T_{15}, in mm.

F_{15} = Average fines content (fraction of sediment sample passing a No. 200 sieve) for granular layers included in T_{15}, in percent.

M = Earthquake magnitude (moment magnitude).

R = Horizontal distance from the seismic energy source, in kilometers (miles multiplied by 1.6).

S = Ground slope, in percent.

T_{15} = Cumulative thickness of saturated granular layers with corrected blow counts, (N1)60, less than 15, in meters (feet multiplied by 0.30)

W = Ratio of the height (H) of the free face to the distance (L) from the base of the free face to the point in question, in percent (Figure 15).

The regression coefficient, r^2, for these models is 83%. The allowable ranges of the independent variables (imputed values) are listed in Table 5. Because there are few measured displacements greater than 10 m (33 ft) in the data set, Equation 5 may not reliably predict values larger than that amount. Extrapolation to values beyond the limits listed in Table 5 yields uncertain predictions. The limits of each independent variable are further discussed in the Section 4.3, entitled Application of Equations.

To show the predictive performance of the above equations, Bartlett and Youd plotted predicted displacements against measured displacements recorded in the observational database (Figure 11). The solid diagonal line on the figure represents perfect prediction, i.e., predicted displacement equals measured displacement. The lower dashed line represents 100% over prediction, and the dashed upper line represents 50% under prediction. Approximately 90% of the data plot between these two dashed bounds. This grouping indicates that predicted displacements are generally valid within a factor of 2 and that doubling of the predicted displacement provides a displacement estimate with a high probability of not being exceeded.

Only a few points plot above the upper dashed line in Figure 11. These points represent lateral spreads where the measured displacement exceeded twice the predicted displacement. Poor quality of subsurface information may be a reason for several of this severe under prediction of displacements at Japanese sites. The one severe under prediction for a U.S. site is from a lateral spread that severely damage the San Fernando Valley Juvenile Hall during the 1971 San Fernando earthquake. An examination of subsurface data from that site revealed that the sediments had some of the highest fines contents in the data set. Those sediments were also locally variable, and probably layered. For the regression analysis, the sediments incorporated in layer T_{15} were characterized by a single average fines content of 59% and single mean grain size of 0.06 mm. If a continuous sublayer of cleaner and coarser sediments passes beneath the site, which appears likely but could not be confirmed from the sparse available data, then a separate analysis of that layer could lead to greater predicted displacement and a smaller degree of over prediction. In addition to the fines content, other factors for this site are at the extremes of the data set. For example, this site is within the crustal uplift zone for the 1971 earthquake, thus the value of R is small and somewhat uncertain. The averaged textural values characterized by an F_{15} of 59% and a D_{50} of 0.06 mm are both beyond the suggested input limits listed in Table 5. Thus, the extrapolation of the model to these conditions contains considerable uncertainty and may be the cause of the severe underprediction.

The over prediction of displacement at a number of sites is less problematic because over prediction may lead to over design, but not generally to unsafe design. Most of the over predicted displacements are for U.S. sites where measured displacements were less than 1 m. These measurements were generally taken near the margins of lateral spreads or on narrow, and in some instances, sinuous lateral spreads, where lateral boundary constraints may have hampered displacement. Thus, Equation 5 may significantly over predict displacements near margins of spreads and at other localities where boundary effects may retard lateral movement.

Equation 5 is generally valid for stiff-soil sites in the Western U.S. or within 30 km of the seismic source in Japan, i.e., the localities from which the case-history data were collected. For these regions and conditions, Equation 5 should be used directly to estimate displacement. For other regions of the world, such as the eastern U.S. where ground motions attenuate more slowly with distance, or for other site conditions, such as liquefiable deposits overlying soft clay layers, where ground motions may be strongly amplified, a correction must be applied to Equation 5 to account for these different conditions.

A preferred method to correct Equation 5 would be to re-regress the model in terms of more flexible parameters, such as M and a_{max}. However, because a_{max} have been measured at only a few lateral spread sites, a direct regression in terms of M and a_{max} is not possible. Attempts by Bartlett and Youd (1992) to developed a regression model based on estimated a_{max} yielded unsatisfactory results (poor correlation coefficients and poor predictions for case-history sites).

As an interim correction measure, until more case history data is assembled which will allow better correlation, Bartlett and Youd (1992) propose the following procedure for estimating displacements for sites with greater peak accelerations than would occur on stiff sites in the western U.S. In this procedure, a corrected distance term, R_{eq}, is applied in Equation 5 in place of the measured distance R. That factor is determined from the curves plotted in Figure 12. Figure 12 shows calculated distances, R_{eq}, at which a given a_{max} occurs for a given earthquake magnitude, M_w, for stiff soil sites in the western U.S. Those R_{eq} were calculated using attenuation equations proposed by Idriss (in press) and soil amplification factors published by Seed et al. (in press).

Specifically, the R_{eq} plotted in Figure 12 were calculated as follows: The peak-acceleration attenuation criteria developed by Idriss were used to calculate peak-acceleration for rock-outcrop sites for a matrix of distances and earthquake magnitudes. A style factor of 0.5 (oblique faulting) was assumed in the attenuation equations. To adjust the rock-outcrop values to stiff site conditions, Bartlett and Youd multiplied the acceleration values calculated for rock sites by a preliminary correction factor estimated from the peak-acceleration amplification curve published by Idriss (1990). More recently, however, Seed et al. (in press) have developed a more rigorous set of amplification curves for a variety of site stiffness conditions (Figure 13), and those curves are used herein. In Figure 13, the curve labeled "C_4+D+E" is approximately the same as the curve suggested by Idriss (1990) for soft soil sites. The curve labeled "B+C_1 to C_3" is a curve Seed et al. (in press) developed for stiff soil sites. Each of the rock-outcrop accelerations estimated from the Idriss criteria were then multiplied by an amplification factor for stiff sites taken directly from curve "B+C_1 to C_3" in Figure 13. The curves in Figure 12 were then compiled by plotting distances at which a given a_{max} occurs on stiff soils for a variety of earthquake magnitudes. The compiled distances were then contoured to give the R_{eq} curves plotted in the figure.

The procedure for using the curves in Figure 12 to correct Equation 5 for non-stiff and non-western U.S. sites is as follows. A design earthquake magnitude, M_w, and peak acceleration, a_{max}, are determined for the candidate site. That magnitude and acceleration are then plotted on Figure 12 and an equivalent source distance, R_{eq}, is interpolated. That R_{eq} is then entered into Equation 5 in place of the actual source distance to calculate the estimated displacement. For example, during the 1989 Loma Prieta, California earthquake (M_w = 6.9), liquefaction and minor lateral spreading with up to 1 ft of displacement were reported on Treasure Island at a distance of about 80 km (48 mi) from the seismic energy source. Application of that distance in Equation 5 along with appropriate soil and site properties indicates that lateral displacement should not have occurred. Considerable ground motion amplification occurred at Treasure Island, however, due to amplification of ground motions through the soft hydraulic fill and San Francisco Bay mud deposits underlying the island. Measured a_{max} on the Island was 0.16 g, whereas maximum bedrock accelerations measured in the area, including a record from Yerba Buena Island just a few thousand feet from Treasure Island, were roughly 0.07 g, and accelerations measured on stiff soil sites in the area were about 0.1 g. Thus, the measured acceleration on Treasure Island was more than twice the bedrock acceleration, and much larger than those on stiff soil sites. Plotting of a magnitude of 6.9 and an a_{max} of 0.16 on Figure 12 gives an R_{eq} of about 40 km (compared to the actual source distance of 80 km). Entering an R_{eq} of 40 km into Equation 5a along with appropriate site and soil properties

yields a predicted lateral displacement of a few tenths of a meter or approximately one foot near the edge of the island. These displacements roughly match the displacements observed following the earthquake.

4.3. APPLICATION OF EQUATIONS.

The general steps for calculating lateral spread displacement are diagrammed on the flow chart in Figure 14. These steps define a procedure for estimating free-field displacements for engineering analyses. Also listed on the chart are the recommended ranges of input values from Table 5, for which predicted displacements have been verified by comparison with the case-history data. Extrapolation beyond those limits, while sometimes allowable, will lead to greater uncertainty in predicted displacements.

4.3.1. Step 1

The first step in estimating lateral ground displacement is to perform a standard analysis of liquefaction susceptibility for the site in question using the procedures outlined in Section 2. If the susceptibility evaluation indicates a factor of safety against liquefaction greater than 1.2 for all granular layers, then lateral displacement should not occur and further analyses of liquefaction and lateral ground displacement are unnecessary. The use of a factor of safety of 1.2 rather than 1.0 adds a margin of safety to account for uncertainty in the liquefaction analysis as noted in Section 2.2 above.

4.3.2. Step 2.

If the analysis in Step 1 indicates a potential for liquefaction at the site, then the evaluation proceeds as follows. $(N_1)_{60}$ values are calculated at incremental depths in each of the saturated granular layers beneath the site. Sufficient SPT or CPT tests should be conducted to adequately characterize each granular layer in the soil profile. Sufficient borings or soundings should be made to adequately define the extent of potentially liquefiable soil layers beneath the area, which may extend well beyond the boundaries of the specific site in question.

The procedure used to calculate $(N_1)_{60}$ is the same as that specified for assessment of liquefaction susceptibility in Section 2. If $(N_1)_{60}$ values equal to or smaller than 15 are not present in granular sediments, then lateral displacements would be small for earthquakes with magnitudes less than 8, and no further analysis is required.

4.3.3. Step 3

If liquefiable sediments, characterized by $(N_1)_{60}$ values less than 15, lie beneath the site, then the analysis proceeds to an evaluation of ground displacement using Equation 5. To apply this analysis, the following seismic, geometric and soil properties are needed.

(1) **Earthquake Magnitude, M.** The same earthquake magnitude, M, should be used in the analysis of lateral displacement as was used in the analysis of liquefaction susceptibility, as stipulated in Section 2.2. Preferably moment magnitude, M_w, should be used in these analyses, but for magnitudes less than 7.5, estimates of either M_s or M_L may be substituted for M_w.

Most of the case history data compiled by Bartlett and Youd (1992) are from earthquakes with magnitudes between 6 and 8. Extrapolation of Equation 5 to magnitudes beyond that range will increase uncertainty in the predicted values. However, because predicted displacement decreases markedly with magnitude, extrapolation to magnitudes smaller than 6 will usually yield small displacements, which, with conservative allowance for the greater uncertainty, are generally useable for engineering analyses. Extrapolation to earthquakes with magnitudes greater than 8 appears to give reasonable predictions of displacement. For example, the predicted displacements agree well with measurements at a few non-gravely sites where displacements were surveyed following the 1964 Alaska earthquake (M_w = 9.2). The amount of data available from these larger events, however, is too meager to provide adequate statistical constraint on the regression analysis. Thus, extrapolation to magnitudes larger than 8 introduces additional uncertainty in the predicted results.

(2) **Seismic Source Distance, R**. The seismic source distance, R, is defined as the horizontal distance in kilometers (miles times 1.6) from the site in question to the nearest point on a surface projection of the seismic source zone. For earthquakes with magnitudes less than 6, the epicentral distances may be an adequate estimate for R. Earthquakes with magnitudes greater than 6, however, are generally associated with a large fault rupture zone that is not adequately characterized by single point such as an epicenter, and epicentral distances should not be used. Source zones for strike-slip and normal faults are commonly delineated by a band incorporating surface ruptures produced by recent (Holocene) faulting events. For these types of faults, which are commonly in the western US, source distances may be measured directly from the edge of the surface rupture zone to the site in question. For reverse faults, shallow-angle thrusts and subduction-zone earthquakes, the associated zone of tectonic crustal uplift generally delineates the surface projection of the seismic source zone. For these types of faults, the source distance is generally measured from the nearest point on the anticipated tectonic uplift zone to the site in question.

For poorly defined earthquake sources or diffuse seismic zones, such as occur in the eastern U.S., the minimal source distances noted in the next section should be used for sites within delineated seismic zones and distances to the edge of the zone should be used for sites outside of the delineated zones.

Because few data from lateral spreads very near the source (small values of R) are included in the database developed by Bartlett and Youd (1992), extrapolation of Equation 5 to small R-distances yields unreliable estimates of lateral displacement. To reduce the possibility of such extrapolation error, Bartlett and Youd suggest a set of lower-limit values for R (Table 6) which should not be subverted in applying Equation 5. Extrapolation below those limits will give uncertain predictions of lateral displacement.

(3) Equation 5 is valid primarily for stiff soil sites in the western U.S. For soft soil sites, where ground motion amplification may occur, or for eastern U.S. sites, where strong ground motions propagate to greater distances than in the west, a correction is required to account for those greater ground motions. That correction is accomplished by correcting the distance term, R, used in equation 5 to R_{eq} by the following procedure. For non-western U.S. sites or for sites with high ground-motion amplification characteristics, R_{eq} is determined from the design seismic factors of magnitude, M, and a_{max} estimated for site in question. The values for these seismic factors would usually be the same as those used in the liquefaction analysis. The required a_{max} is plotted against magnitude on Figure 12, and the equivalent source distance, R_{eq} is interpolated from the R_{eq}-curves. The derived R_{eq} is then used in Equation 5. This procedure is only valid for a_{max} less than about 0.4 g and earthquake magnitudes less than 8. Extrapolation beyond these values will lead to less certain predictions.

As an example, assume that an eastern U.S. earthquake of magnitude 7.5 is estimated to produce an a_{max} of about 0.20 g at a source distance of 90 km (54 mi). By plotting an a_{max} of 0.20 g against a magnitude, M, of 7.5 on Figure 12, an R_{eq} of about 42 km is determined. The 42-km value is then applied as the R-value in equation 5.

(4) **Free-Face Ratio, W**. The definition of free-face ratio and the measurements required to calculate this parameter are illustrated in Figure 15. The height of the free face, H, is defined as the vertical distance between the base and the crest of the free-face. That height is commonly determined by subtracting the elevation at the base, such as at the base of a river bank or at the toe of a fill, from the elevation at the top of the slope, such as at the top of a river bank or crest of an embankment. The distance, L, is measured from the base or toe of the free face to the locality in question. The free-face ratio, W, is then calculated from the relationship:

$$W = (H/L)(100), \text{ in percent} \qquad (6)$$

Most values of W in the data set complied by Bartlett and Youd (1992) lie between 1% and 20 %. Extrapolation to values beyond that range will lead to great uncertainty in predicted displacements. For free-face ratios greater than 20%, gravitational forces may be sufficiently large for liquefaction to trigger either a flow failure or a rotational slump. In either instance, displacements may be much larger than those predicted by Equation 5a.

Free-face ratios less than 1% generally lead to small predicted displacements which may be used with conservatism for flat ground conditions. However, in areas of sloping terrain, calculations should also be made using Equation 5b for sloping ground conditions. The larger of the two calculated displacements should be utilized for design or other applications.

(5) **Slope, S**. The ground slope, S, corresponds to the standard engineering definition of slope, that is the rise of elevation over the horizontal run of the slope (Figure 15). For a unit rise of elevation, say 1 ft (or 1 m) over a horizontal distance of X ft (or X m), the slope is:

$$S = (1/X)(100), \text{ in percent} \qquad (7)$$

Where both sloping ground and a free face may affect lateral ground displacement at a site, calculations should be made using both Equations 5a and 5b. The larger of these two predictions should be used to estimate the ground displacement.

Ground slopes in the database compiled by Bartlett and Youd (1992) range from 0.1 to about 6%. Extrapolation beyond this range will lead to uncertain predictions. For slopes less than 0.1%, chaotic displacements due to ground oscillation are likely to exceed those from lateral spread. Thus, Equation 5 may give uncertain estimates of lateral displacement for flat ground conditions. Ground slopes that exceed 6% may be subject to flow failure and consequent large displacements. Equation 5 is not valid for estimating flow-failure displacements.

(6) **Thickness of loose granular sediment, T_{15}**. The thickness of loose granular layers in the sediment cross section is an important factor controlling amount of lateral ground displacement at liquefaction sites. Bartlett and Youd (1992) define that parameter as the thickness of granular layers in a sediment profile characterized by an $(N_1)_{60}$ equal to or less than 15. Figure 5 illustrates the

determination of T_{15}. That figure shows $(N_1)_{60}$ plotted against depth along with a dashed line marking an $(N_1)_{60}$ of 15. A stippled band paralleling the dashed line indicates depths where $(N_1)_{60}$ is less than 15. There are several possible choices for defining T_{15} for this illustration:

(a) One could sum the intervals marked by the stippled band shown on the figure. That interpretation yields two segments of sediment characterized by $(N_1)_{60}$ less than 15, a segment between depths of 5 ft and 11 ft, and a second segment between depths of 14 ft and 20 ft. The total length of these two segments is 12 ft. That length, when applied in Equation 5, would yield a smaller estimated displacements than the choices noted below. That smaller estimate may underestimate the displacement that is most likely to occur. Thus, this option is an unsafe option.

(b) Because only one $(N_1)_{60}$ value exceeds 15 in the depth interval between 5 ft and 20 ft, for conservative design that value should be disregard in determining T_{15}. That $(N_1)_{60}$ may have been anomalous (the penetrometer may have hit a stone or other obstruction) or the reading may have been erroneous. Even if the $(N_1)_{60}$ is correct, the factor of safety against liquefaction is only slightly greater than unity, indicating that the soil at the depth in question could soften and participate to some degree in ground deformation. If two or more consecutive tests yield $(N_1)_{60}$ greater than 15, then a denser layer is more certain, and the intervening depth segment may be excluded from T_{15}. Finally, because a larger displacement is calculated by including the questionable segment than omitting it, that segment should be included in T15 to be conservatively safe. Using this option, thickness T_{15} is defined as 15 ft, which includes all the sediment between depths of 5 and 20 ft.

(c) Two layers with distinctly different textures are incorporated in T_{15} as defined above, a sand to silty sand between depths of 5 ft and 17 ft, and a silty sand between depths of 17 ft and 20 ft. Combining of these two layers, which requires averaged soil properties for the analysis, leads to smaller estimated displacements than when the layers are considered separately. Thus for conservative design, the two layers should be defined separately; analyses using Equation 5 should made for each layer; and the predicted displacements from the separate analyses summed to provide the final estimate of displacement.

An examination of the soil stratigraphy illustrated in Figure 5 suggests that a further definition of layers might be considered to separate the sand (SW), between 5 ft and 11 ft, from the sand to silty sand (SW-SM), between 11 ft and 17 ft. Because the textural differences between these layers are not great, the latter separation would make only a small difference (but a slight increase) in the estimated displacement. Thus, whether or not to make this additional separation is a matter of engineering judgement. However, for this method of analysis, sublayers should not be defined unless there are significant textural differences between the sublayers.

For soil layers composed of thinly laminated materials (sublayers less than one foot thick) or thinly interbedded sediments, T_{15} should be defined as the total thickness of the layer rather than the thinner sublayers, and the soil properties (F_{15} and $D50_{15}$) should be averaged over the entire layer.

One additional aspect of the calculation of T_{15} is illustrated by the soil profile depicted in Figure 5. There is a marginally liquefiable layer between depths of 23 ft and 32 ft, with factors of safety against liquefaction ranging from 0.92 to 1.42. $(N_1)_{60}$'s over that same interval range from 15.9 to 17.7. Because these $(N_1)_{60}$'s exceed 15, this layer need not be included in T_{15}.

Although not shown on the soil profile illustrated in Figure 5, some granular soil layers in a soil profile may be characterized by an $(N_1)_{60}$ less than 15, and yet have a factor of safety against liquefaction greater than 1.2. This condition commonly occurs at sites subjected to low levels of earthquake shaking. Such non-liquefiable layers should not to be included in T_{15}.

The thicknesses, T_{15}, in the case history data compiled by Bartlett and Youd range from 0.3 m to 15 m (1 ft to 50 ft). Extrapolation beyond that range will lead to uncertain predictions. Extrapolation to thickness less than 0.3 m (1 ft), however, should generally yield relatively small estimated displacements. Conservative assessment of displacement based on these predictions may be used for engineering analysis.

Liquefiable granular layers with thicknesses greater than 15 m (50 ft) are unusual in natural sediments. Extrapolation of Equation 5 to these unusual thicknesses will add uncertainty to the predicted displacements. Because it is unlikely that the entire thickness of such a layer would participate equally in producing ground displacement, the predicted displacements are likely to be greater than actual displacements. Such predictions may be used with engineering judgement for estimating conservative displacements for routine design applications.

(7) **Average fines content, F_{15}.** The regression analysis of Bartlett and Youd (1992), indicates that fines content, the percentage of material in a soil passing the No. 200 sieve (finer than 0.074 mm), is a major factor affecting the lateral ground displacement. Equation 5 indicates that the greater the fines content, the smaller the displacement of lateral spreads, all other factors remaining equal. To characterize the fines content of a liquefiable soil, Bartlett and Youd introduced the term F_{15} which is defined as the average fines content of materials included in a layer T_{15}. For example, referring to Figure 5, the F_{15} for sand to silty-sand layer between depths of 5 and 17 ft would be the average of the fines contents from tests on four individual samples taken from that layer as listed in Table 5, or:

$$F_{15} = (3\% + 5\% + 10\% + 8\%)/4 = 6.5\%$$

If that layer were to be divided into two sublayers (from 5 ft to 11 ft, and 11 ft to 17 ft) then the F_{15} for the upper layer would be 4%, and the F_{15} for the lower layer would be 9%.

As noted in the previous section, because of the large difference in fines content for this illustration between the silty sand (SM) compared to the overlying cleaner sands, a separate T_{15} layer should be defined for the silty sand (17 ft to 20 ft depth). Because only one sample was taken from that layer, the average fines content, F_{15}, for that layer is estimated as 43%.

Most of the F_{15} estimates in the data set compiled by Bartlett and Youd (1992) are between 0 and 50%. Extrapolation to fines contents greater than 50 percent leads to uncertain predictions.

(8) **Average mean-grain size, $D50_{15}$.** The regression analysis by Bartlett and Youd (1992) shows that lateral ground displacement generally decreases with increased coarseness of the liquefiable material. They characterized that coarseness by a parameter, $D50_{15}$, which is the average mean-grain size of materials included in layer T_{15}. For example, for the sand to silty sand layer between depths of 5 ft and 17 ft as illustrated on Figure 5, the average mean grain size is:

$$D50_{15} = (0.43 \text{ mm} + 0.51 \text{ mm} + 0.31 \text{ mm} + 0.37 \text{ mm})/4 = 0.405 \text{ mm}$$

For the underlying silty sand layer, $D50_{15}$ is approximated by the single measured mean-grain size of 0.11 mm.

The mean-grain sizes, $D50_{15}$, for which Equations 4 is valid, ranges from 0.1 mm to 1.0 mm. Data in the case histories do not support extrapolation of $D50_{15}$ for granular soils to values beyond this range. Extrapolation to finer grained soils adds uncertainty to the predicted values; these values, however, are generally small and may be used with caution for ordinary design. However, if the finer-grained soils are collapsible or have sensitivities greater than about 1.5, displacements may be large and Equation 5 should not be applied. Extrapolation to mean grain sizes greater than 1 mm adds great uncertainty to the predicted displacements. For example, comparison of measured and predicted displacements from sites where liquefaction of coarse grained materials has occurred in past earthquakes, yields estimated and measured values that vary greatly and randomly from each other. Factors not incorporated in Equation 5, such as soil permeability, apparently greatly affect lateral displacements in coarse grained materials, and render Equation 5 invalid for estimating displacements for these types of materials.

In addition to the specified limits on the values of F_{15} and $D50_{15}$ for which Equation 5 is valid, there are also is limits on allowable combinations of these values. Figure 16 shows a plot of F_{15} versus $D50_{15}$ for all of the data in the database compiled by Bartlett and Youd (1992). This plot shows a rather narrow band of combinations of F_{15} and $D50_{15}$ for which Equation 5 is valid. Extrapolation beyond these textural limits introduces uncertainty into the predicted displacements.

4.3.4. Further Restrictions on Use of Equation 5

Equation 5 was regressed from observed displacements at previous lateral spread sites. Most of those sites were located in areas underlain by broad deposits of liquefiable soil. In those few instances where data were collected from lateral spreads that traversed narrow or sinuous channels, displacements were generally much smaller than those predicted by Equation 5. For example, the lateral spreads that developed in the South of Market and Mission Creek zones of San Francisco during the 1906 earthquake moved only about 10% to 20% of the distance predicted by Equation 5. In those instances, nearby lateral boundaries apparently impeded displacement. Similarly, near the edge (boundary) of a lateral spread, displacements are likely to be significantly reduced by lateral boundary effects compared to displacements in the main body of the spread (see circled data on Figure 11). Thus, Equation 5 may greatly over predict lateral displacements in narrow spread zones or near the boundaries of wider zones.

4.4. EXAMPLE CALCULATIONS.

To illustrate the calculation of lateral ground displacement using Equation 5, consider the hypothetical soil stratigraphy and ground conditions shown on Figure 17. Soil properties for the various layers are listed in Table 3 and plotted on Figure 5. This cross section depicts soil layers beneath a possible site for a large radar tower. The foundation for the tower is to be constructed with steel piles that could withstand up to 3 ft of lateral displacement without impairment of their ability to support the radar tower.

The design earthquake magnitude, source distance and peak acceleration specified by engineering seismologists for this site are 6.5, 11 km, and 0.30 g, respectively. The site is a stiff soil site in the western U.S. The other parameters required for application of Equation 5 are determined as follows:

From the cross section of the site, the height of the free face (channel depth) is noted as 16 ft. The planned tower is located 150 ft from the base of the free face. Thus, W = (16 ft/150 ft)(100) = 10.7%. The gentle ground slope of the terrain at the tower site has is characterized by a rise of elevation of 1.0 ft over a distance of 200 ft yielding a ground slope, S, of 0.5%.

The soil stratigraphy and soil properties were defined in previous examples and the results noted on Figure 5. From a review of Figure 5 and the soil-property data in Table 3, the liquefiable layer is divided into two sublayers: Layer 1 is composed of sand to silty sand with a thickness, T_{15}, of 12 ft (3.6 m), an average fines content, F_{15}, of 6.5%, and an average mean-grain size, $D50_{15}$, of 0.405 mm. Layer 2 is composed of silty sand with a T_{15} of 3 ft (0.9 m), F_{15} of 43, and $D50_{15}$ of 0.11 mm. Application of those parametric values Equations 5a and 5b yields the following results:

For free-face conditions:

For layer 1,

$$\text{Log } D_{H1} = -16.366 + 1.1782\,(6.5) - 0.9275\,\text{Log}(11\text{ km}) - 0.0133(11\text{ km}) + 0.6572\,\text{Log}(10.7\%) + 0.3483\,\text{Log}(3.7\text{ m}) + 4.527\,\text{Log}(100 - 6.5\%) - 0.9224\,(0.405\text{ mm}) = -0.3972$$

and, $D_{H1} = 0.40$ m (1.34 ft)

For layer 2,

$$\text{Log } D_{H2} = -16.366 + 1.1782\,(6.5) - 0.9275\,\text{Log}(11\text{ km}) - 0.0133(11\text{ km}) + 0.6572\,\text{Log}(10.7\%) + 0.3483\,\text{Log}(0.9\text{ m}) + 4.527\,\text{Log}(100 - 43\%) - 0.9224\,(0.11\text{ mm}) = -1.3119$$

and, $D_{H2} = 0.05$ m (0.16 ft)

The total free-face displacement is the sum of the component displacements:

$$D_H = 0.40\text{ m} + 0.05\text{ m} = 0.45\text{ m}\ (1.50\text{ ft})$$

For ground slope conditions:

For Layer 1,

$$\text{Log } D_{H1} = -15.787 + 1.1782\,(6.5) - 0.9275\,\text{Log}(11\text{ km}) - 0.0133(11\text{ km}) + 0.4293\,\text{Log}(0.5\%) + 0.3483\,\text{Log}(3.7\text{ m}) + 4.527\,\text{Log}(100 - 6.5\%) - 0.9224\,(0.405\text{ mm}) = -0.6239$$

and, $D_{H1} = 0.24$ m (0.80 ft)

For layer 2,

$$\text{Log } D_{H2} = -15.787 + 1.1782\,(6.5) - 0.9275\,\text{Log}(11\text{ km}) - 0.0133(11\text{ km}) + 0.4293\,\text{Log}(0.5\%) + 0.3483\,\text{Log}(0.9\text{ m}) + 4.527\,\text{Log}(100 - 43\%) - 0.9224\,(0.11\text{ mm}) = -1.5387$$

and, $D_{H2} = 0.03$ m (0.10 ft)

The total ground slope displacement is the sum of the component displacements:

$$D_H = 0.24\text{ m} + 0.03\text{ m} = 0.27\text{ m } (0.90\text{ ft})$$

Only the larger of the two estimated displacements need be used in the design analysis. In this instance that displacement is 1.5 ft. (If the designer wished to be ultraconservative, the displacements predicted for ground-slope conditions could be added to the free-face displacement. That degree of conservatism, however, is not required.)

The calculated displacement of 1.5 ft is less than the allowable displacement of 3.0 ft, indicating that the tower foundation is safe for the mean expected displacement. Because the tower supports an important radar scanning device, however, it may be classed as a critical structure, requiring a displacement with a high probability of not being exceeded. Based on Figure 11, doubling of the displacement predicted by Equation 5 yields a value with a high probability of not being exceeded. In this instance the predicted displacement of 1.5 ft should be doubled to 3.0 ft for conservative design. This estimated displacement of 3 ft is equal to the 3 ft of allowable displacement, and the structure is only marginally safe against liquefaction-induced lateral spreads that could be generated by the design earthquake.

Section 5. REFERENCES

1. Ambraseys, N.N., 1988, Engineering Seismology, Earthquake Engineering and Structural Dynamics, Vol. 17, No.1, p. 1-105.

2. Bartlett, S.F., and Youd, T.L., 1992, Empirical analysis of horizontal ground displacement generated by liquefaction-induced lateral spread: National Center for Earthquake Engineering Research, Technical Report NCEER-92-0021.

3. BSSC, 1991, NEHRP Recommended Provisions for the Development of Seismic Regulations for New Buildings, Building Seismic Safety Council, Chapter 7 Commentary, p. 151-163.

4. Byrne, P..M., Jitno, H., and Salgado, F., 1992, Earthquake Induced Displacement of Soil-Structures Systems, Proceedings, 10th World Conference on Earthquake Engineering, Madrid, Spain, p. 1407-1412.

5. Finn, W.E.L., and Yogendrakumar, M., 1989, TARA-3FL: Program for Analysis of Liquefaction Induced Flow Deformations, Department of Civil Engineering, University of British Columbia, Vancouver, B.C., Canada

6. Idriss, I.M., 1990, Response of Soft Soil Sites During Earthquakes, Proceedings, H. Bolton Seed Memorial Symposium, Vol. 2, BiTech Publishers, LTD, Vancouver, B.C. Canada, p. 273-290.

7. Idriss, I.M., in press, Procedures for Selecting Earthquake Ground Motions at Rock Sites, A Report to the National Institute of Standards and Technology, U.S. Dept. of Commerce, Gaithersburg, Maryland.

8. Kulhawy, F.H., and Mayne, P.W., Manual on Estimating Soil Properties for Foundation Design, Electric Power Research Institute, Palo Alto, CA, Report EPRI EL-6800.

9. NRC, 1985, Liquefaction of Soils During Earthquakes, National Research Council, National Academy Press, Washington, D.C., 240 p.

10. Newmark, N.M., 1965, Effects of Earthquakes on Dams and Embankments, Geotechnique, Vol. 15, No. 2, p. 139-160.

11. Prevost, J.H., 1981, DYNA-FLOW: A Nonlinear Transient Finite Element Analysis Program, Report No. 81-SM-1, Department of Civil Engineering, Princeton University, Princeton, NJ.

12. Seed, H.B., and Idriss, I.M., 1982, Ground Motions and Soil Liquefaction During Earthquakes, Earthquake Engineering Research Institute, Monograph, 134 p.

13. Seed, H.B., Idriss, I.M., and Aarango, I., 1983, Evaluation of Liquefaction Potential Using Field Performance Data, Journal of the Geotechnical Engineering Division, ASCE, Vol 102, No. GT4, p. 246-270.

14. Seed, H.B., Tokimatsu, K., Harder, L.F., and Chung, R.F., 1985, Influence of SPT Procedures in Soil Liquefaction Resistance Evaluations, Journal of the Geotechnical Engineering Division, ASCE, Vol 111, No. 12, p. 1425-1445.

15. Seed, R.B., Dickenson, S.E., Rau, G.A., White, R.K., and Mok, C.M., in press, Observations Regarding Seismic Response Analyses for Soft and Deep Clay Sites, Proceedings, Workshop on Site Response During Earthquakes and Seismic Code Provisions, National Cent. for Earthquake Engr. Resch./ Structural Engrs. Assn. of Calif., November 18-20, 1992.

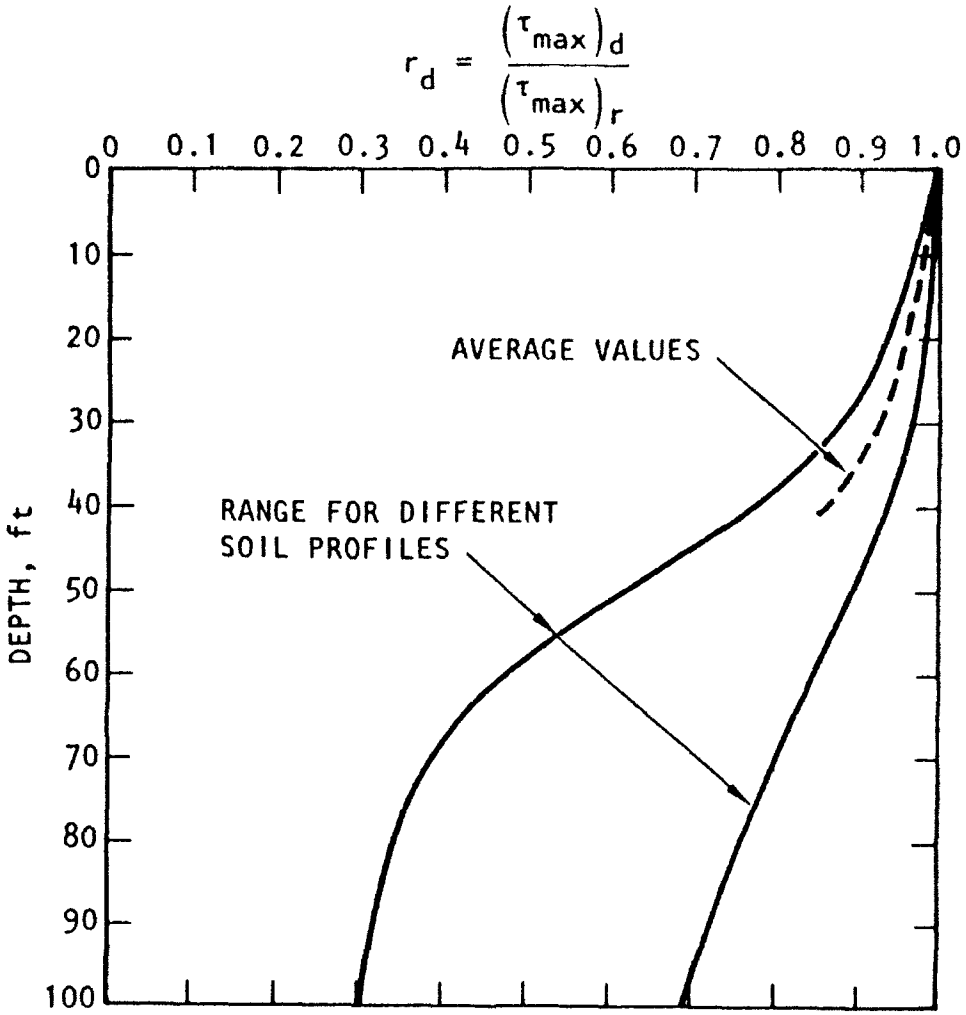

FIGURE 1

Range of r_d for Different Soil Profiles and Sediment Depths
(After Seed and Idriss, 1982)

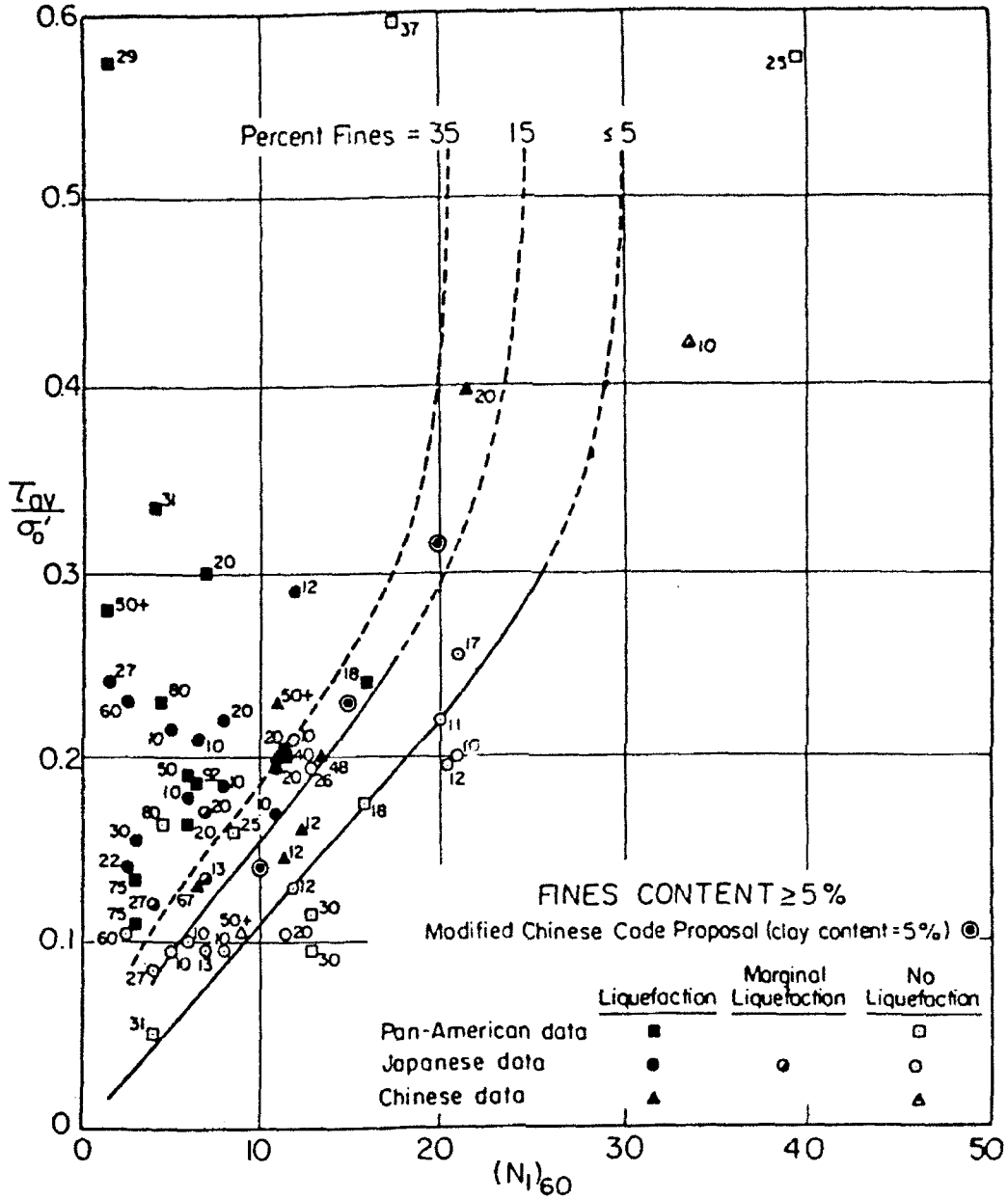

FIGURE 2

Relationship between CSRL and $(N_1)_{60}$ for Sands and Silty Sands and Magnitude 7.5 Earthquakes (After NRC, 1985)

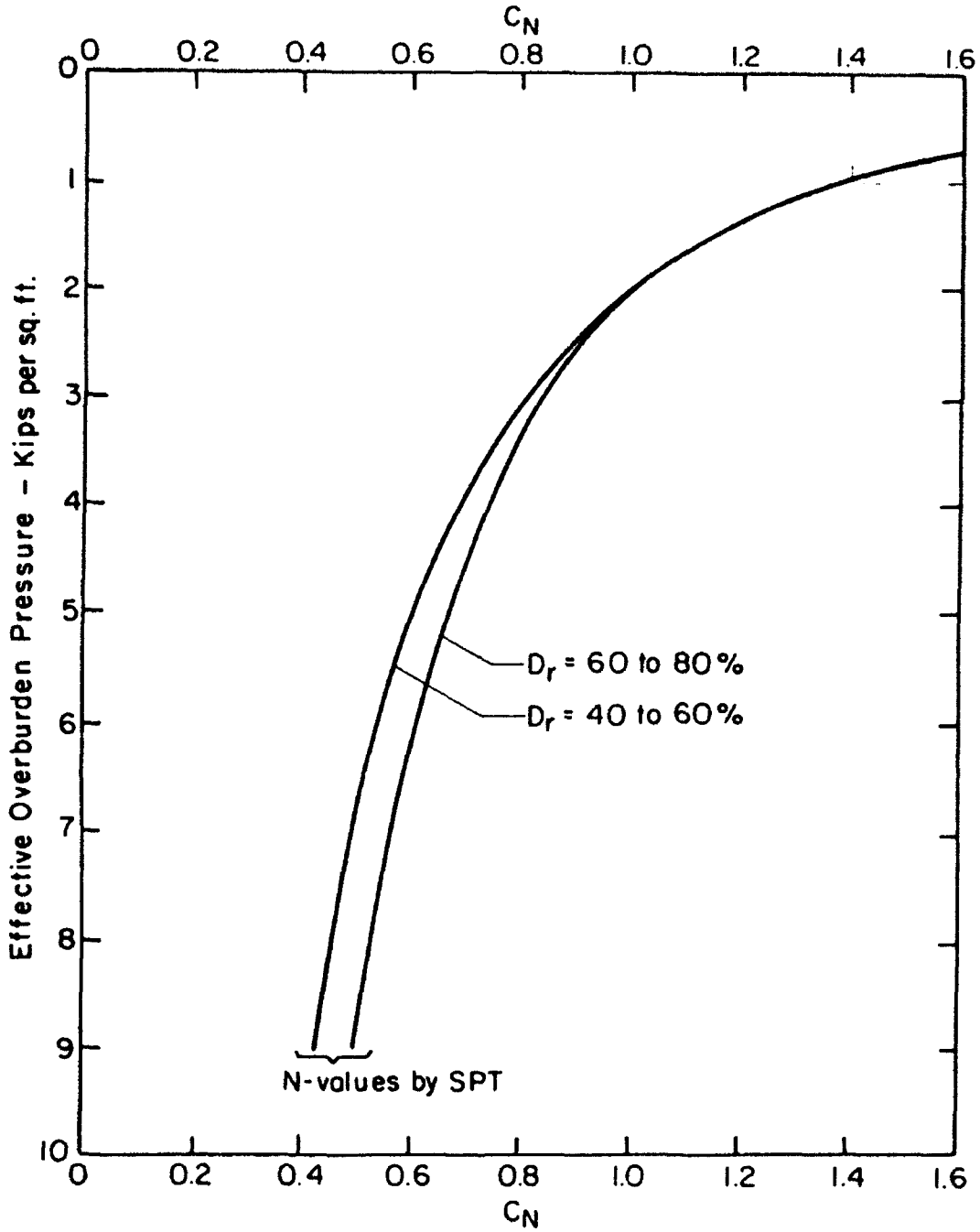

FIGURE 3

Relationship Between Correction Factor, C_N, and Effective Overburden Pressure, σ_v'
(After NRC, 1985)

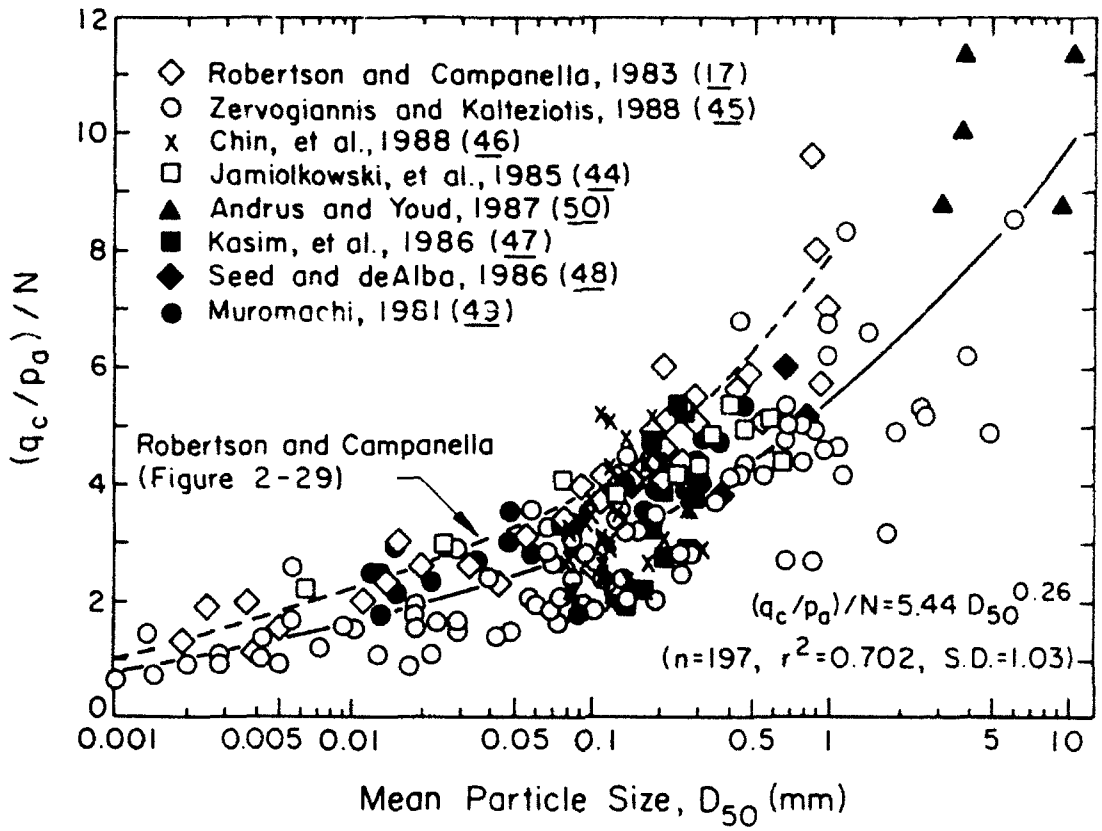

FIGURE 4

Recommended Variation of q_c/N with Grain Size for Fugro Electric Friction Cones
(After Kulhawy and Mayne, 1990)

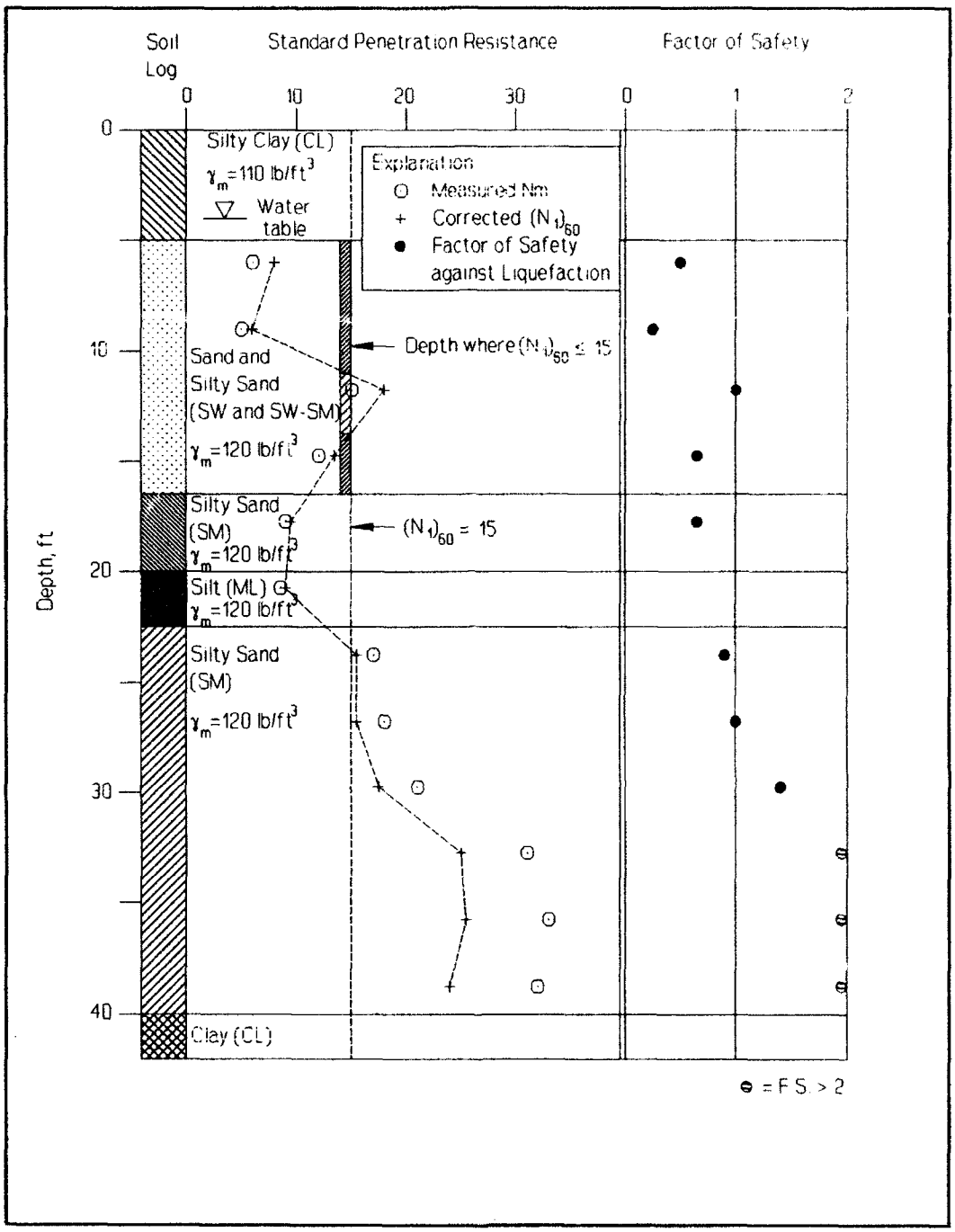

FIGURE 5

Hypothetical Soil Profile For Example Calculations

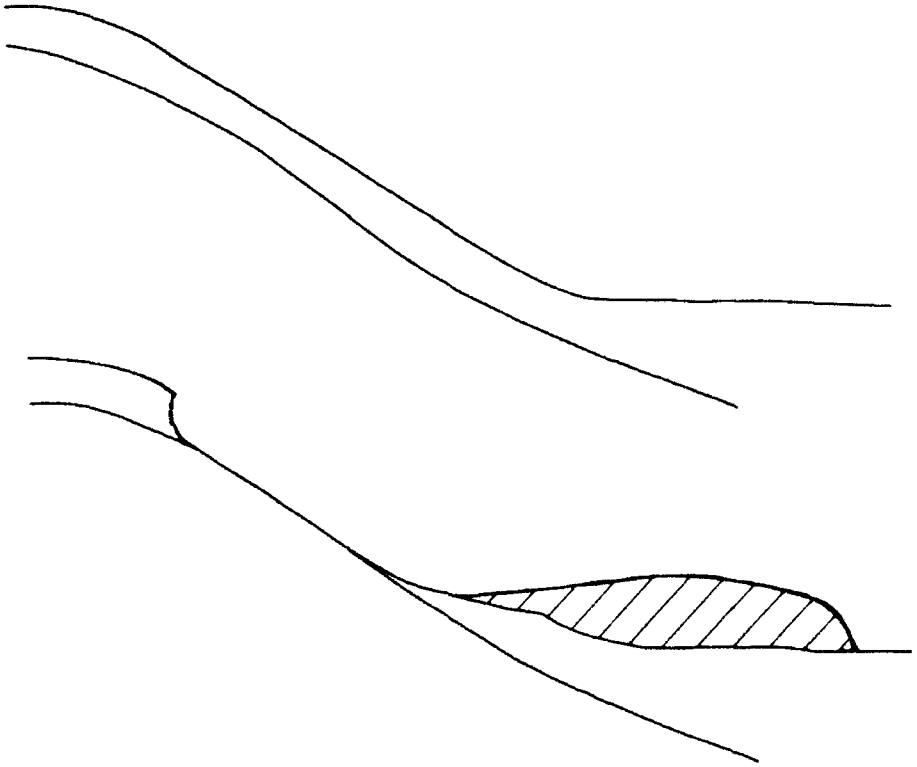

FIGURE 6

Illustration of Flow Failure Caused by Liquefaction, Loss of Soil Strength, and Massive Down Slope Movement of Liquefied Material
(After NRC, 1985)

FIGURE 7

Flow Failure Along Shoreline of Lake Merced, San Francisco, California
Triggered by Liquefaction During the 1957 Daly City Earthquake
(U.S. Geological Survey Photograph)

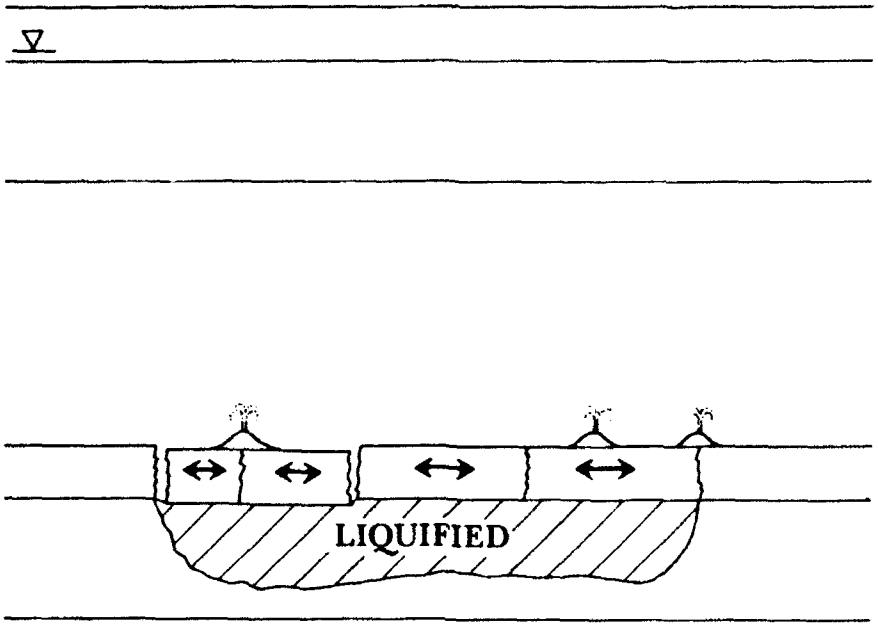

FIGURE 8

Illustration of Ground Oscillation Caused by Liquefaction Decoupling Surface Soil Layers Oscillate in Waves in Response to Earthquake Shaking
(After NRC, 1985)

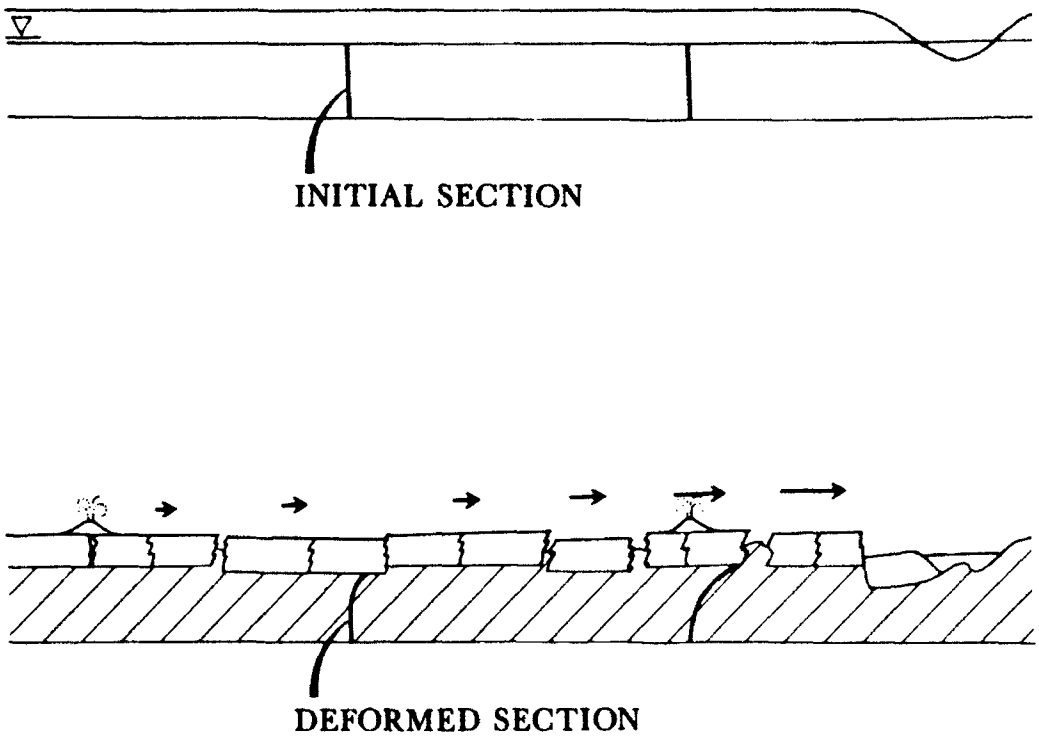

FIGURE 9

Illustration of Lateral Spread Showing Displacement of Ground Surface Down Mild Slope or Toward a Free Face as a Consequence of Liquefaction of a Subsurface Soil Layer (After NRC, 1985)

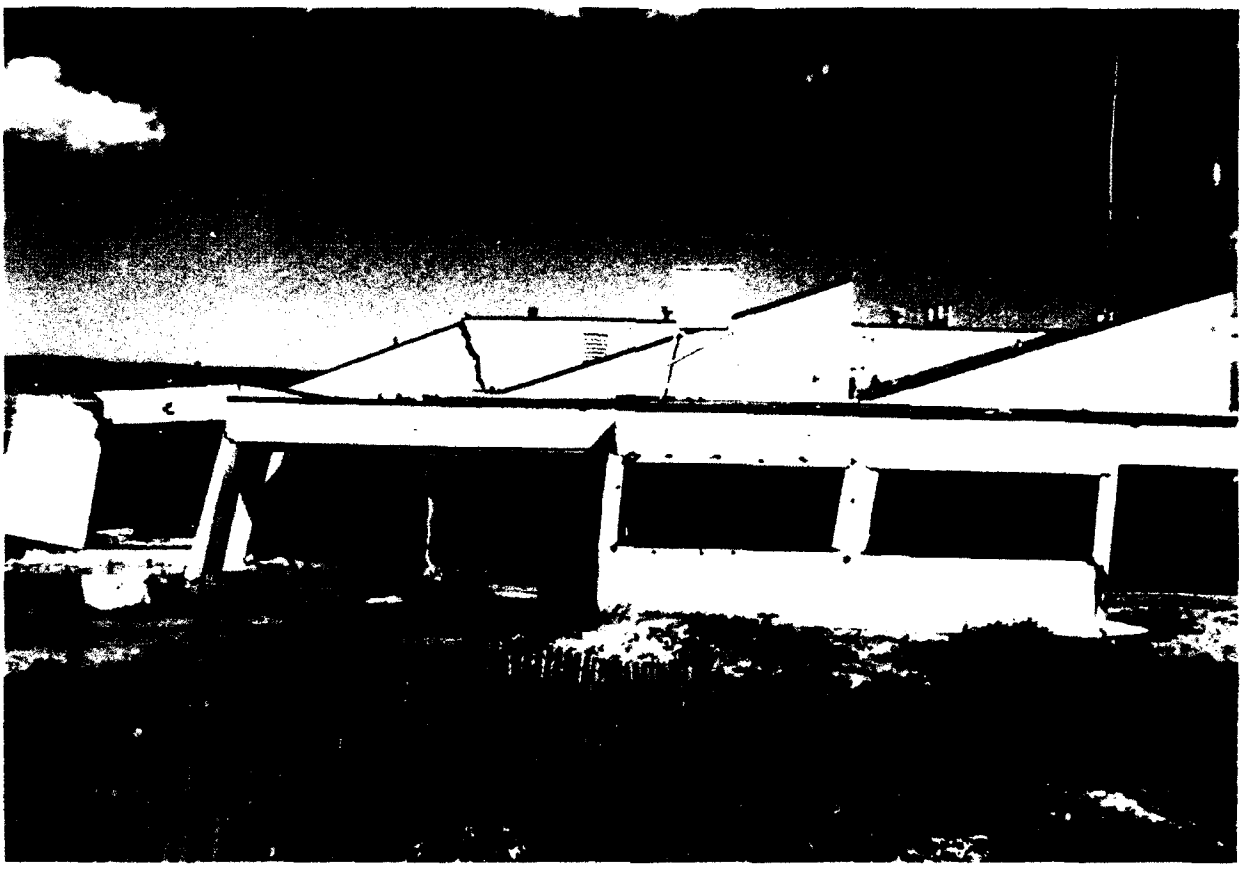

FIGURE 10

Marine Science Laboratory Pulled Apart by a Few Feet of Lateral Spread Displacement During 1989 Loma Prieta, California Earthquake (Photograph by S.F. Bartlett, Brigham Young University)

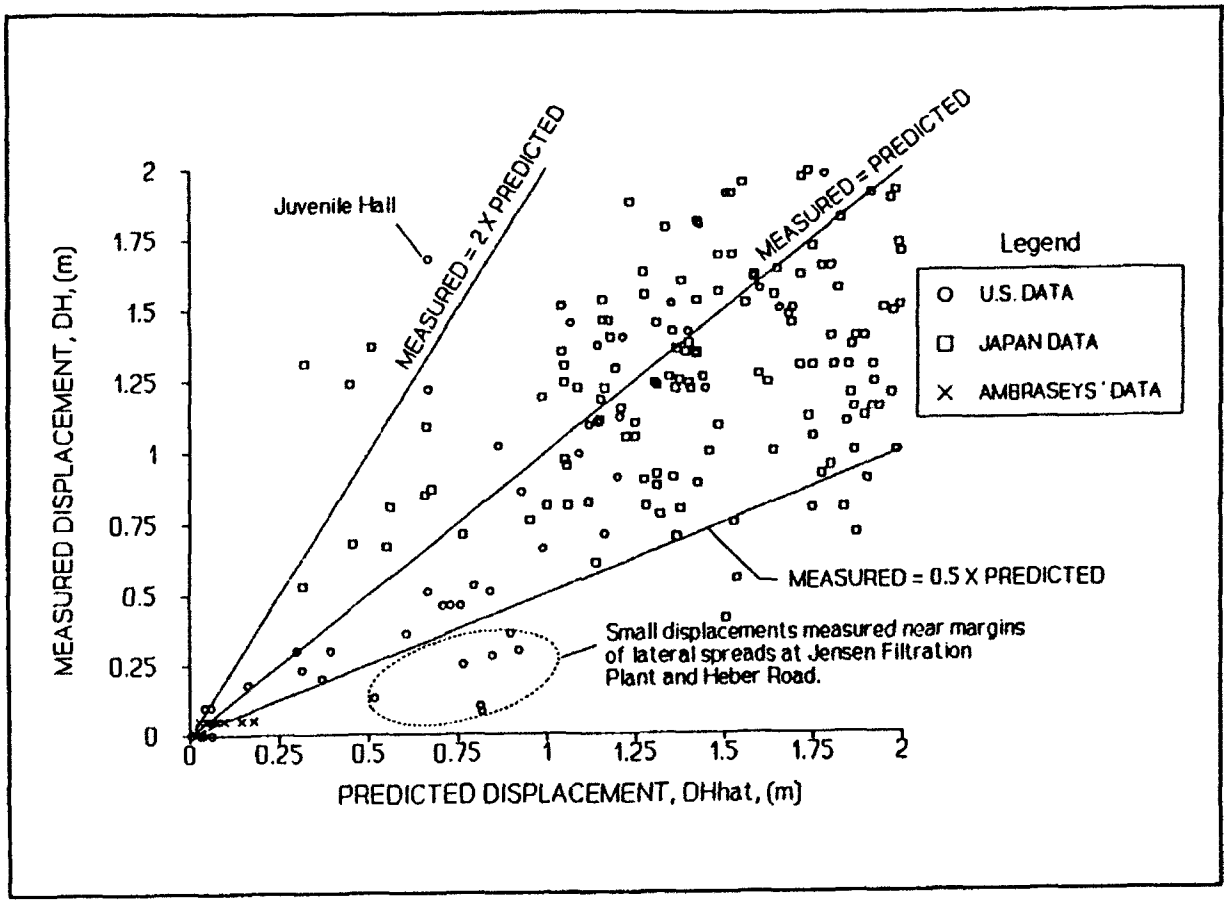

FIGURE 11

Measured Versus Predicted Displacements Using Equation 5 and Case History Lateral Spread Sites (After Bartlett and Youd, 1992)

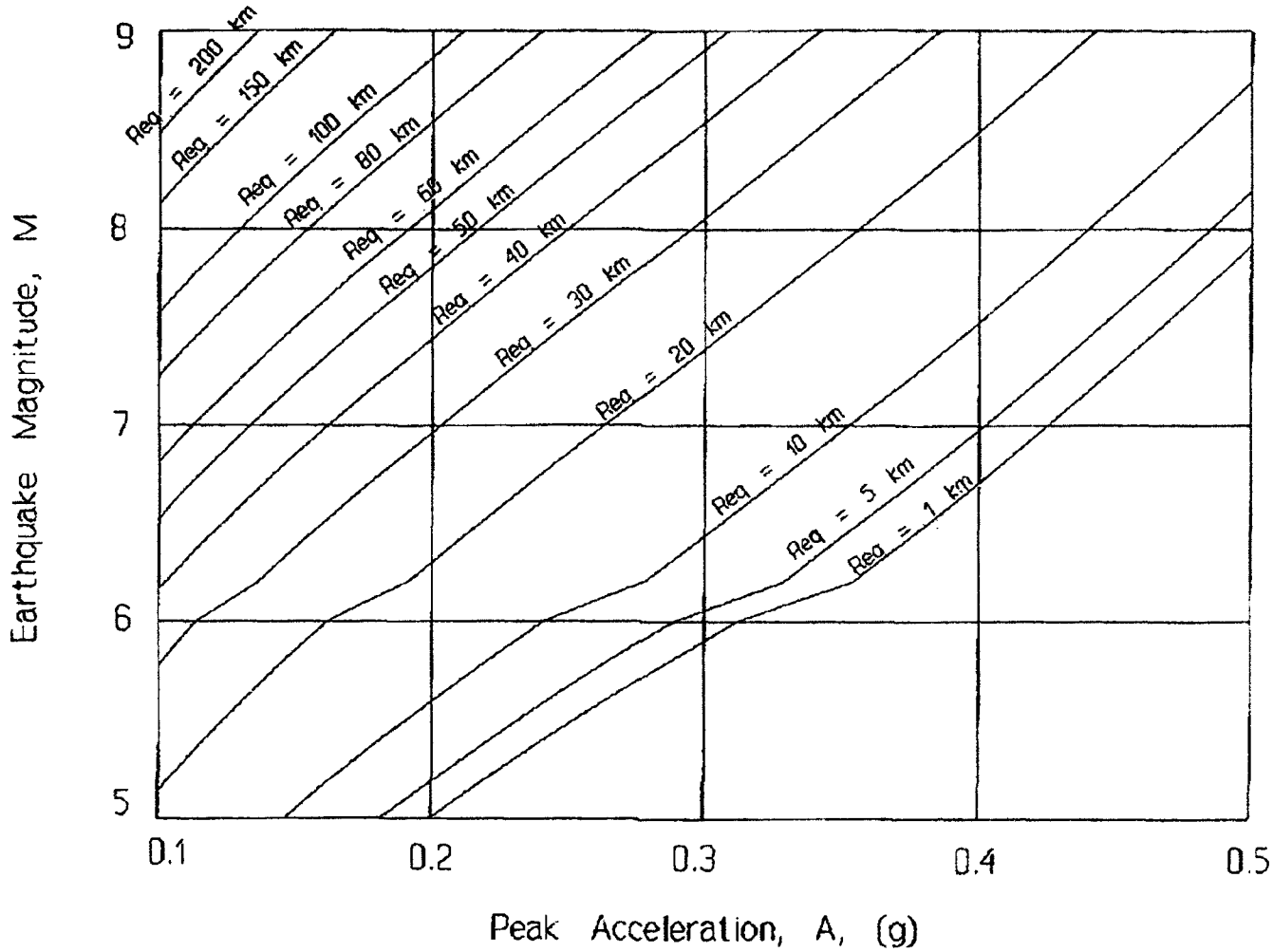

FIGURE 12

Graph for Determining Equivalent Source Distance, R_{eq}, From Magnitude and a_{max}
(After Bartlett and Youd, 1992)

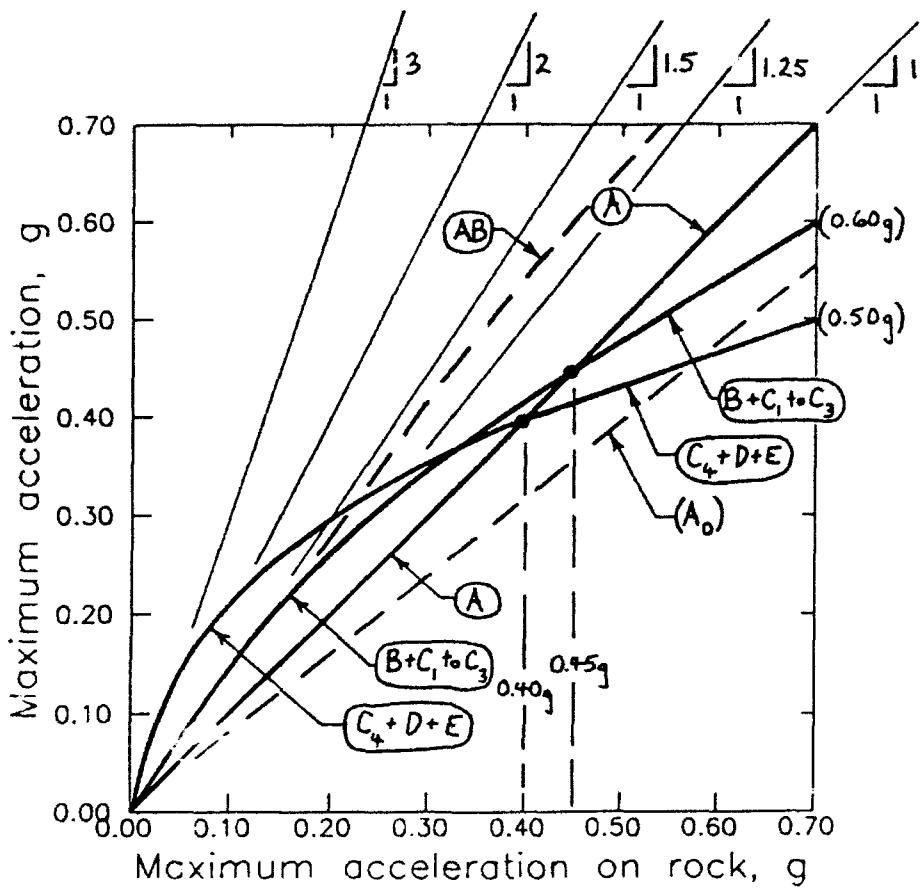

FIGURE 13

Approximate Curve for Estimating a_{max} for Stiff Soil Sites

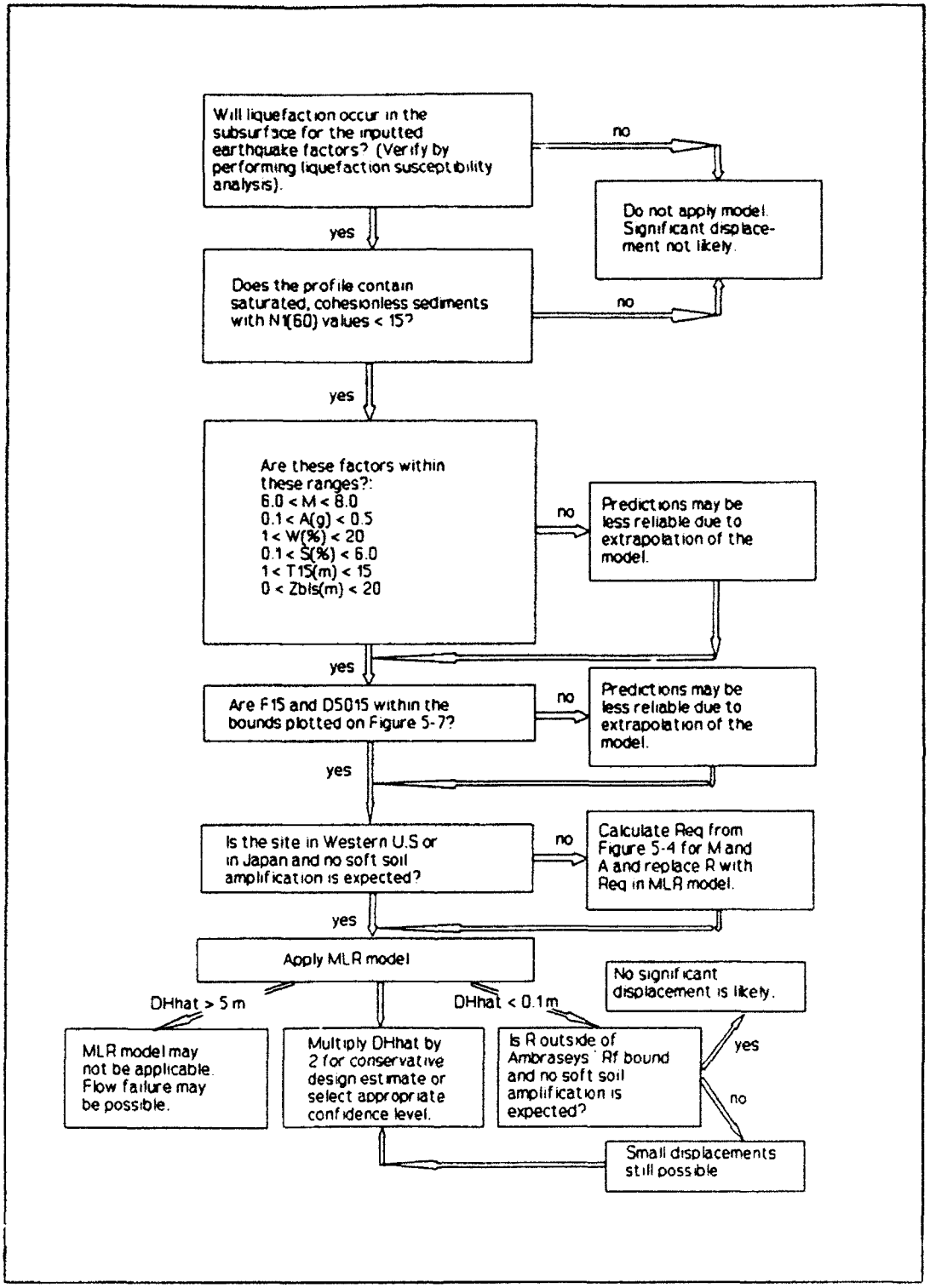

FIGURE 14

Flow Chart For Application of Equation 5

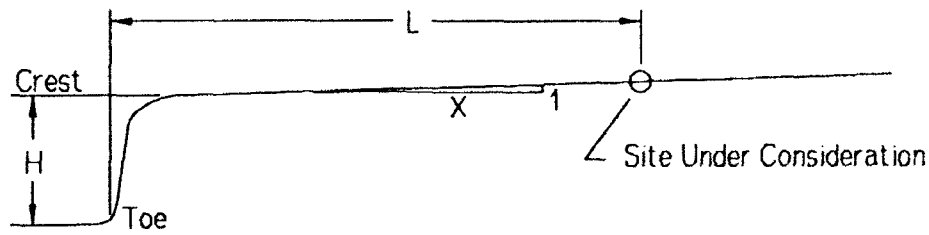

L = Distance From Toe Of Free Face To Site Under Consideration
H = Height Of Free Face (Crest Elev. - Toe Elev.)
W = Free-Face Ratio = (H/L)(100), in percent
S = Slope Of Natural Ground Toward Channel = 1/X*100, in percent

FIGURE 15

Definitions for Slope, S, and Free-Face Ratio, W

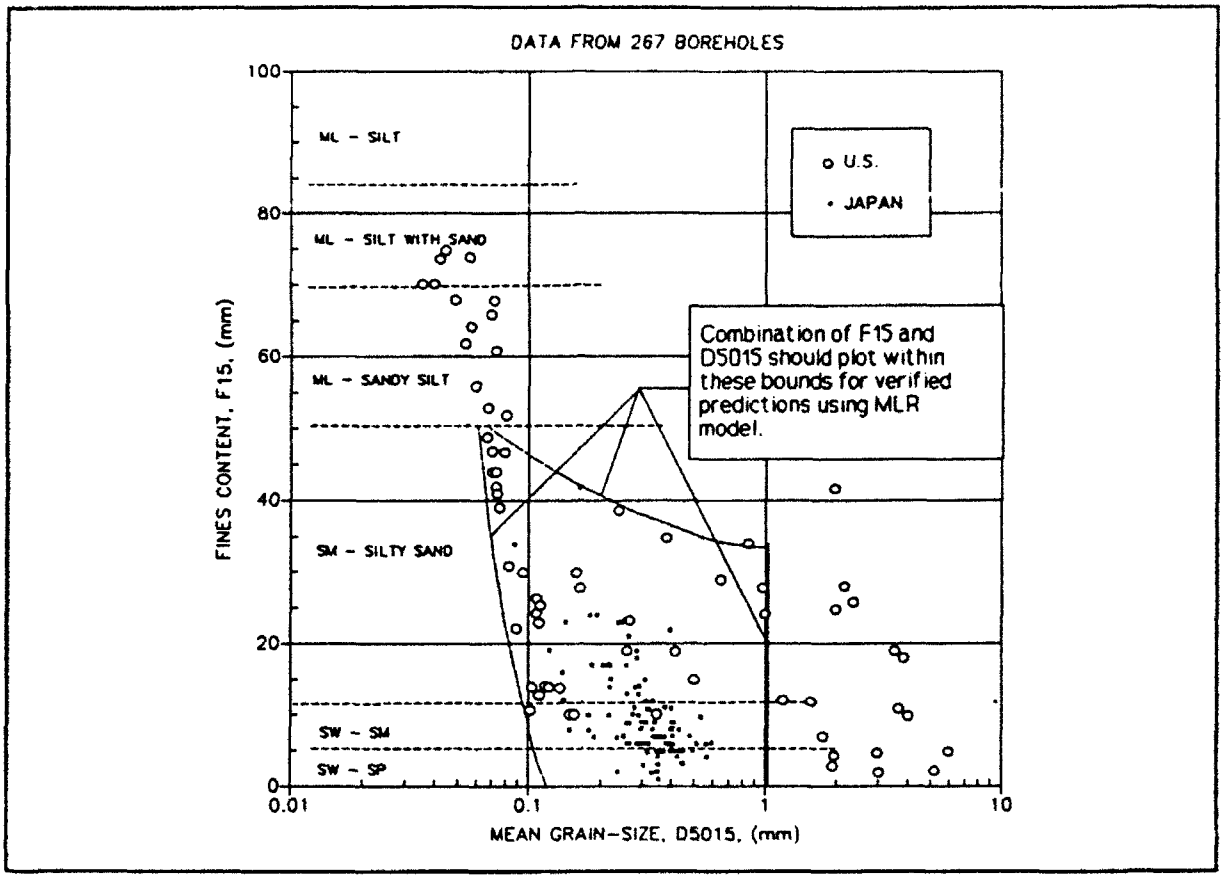

FIGURE 16

Plot of F_{15} Versus $D50_{15}$ From Case History Database and Bounds Beyond Which Equation Will Give Uncertain Results (After Bartlett and Youd, 1992)

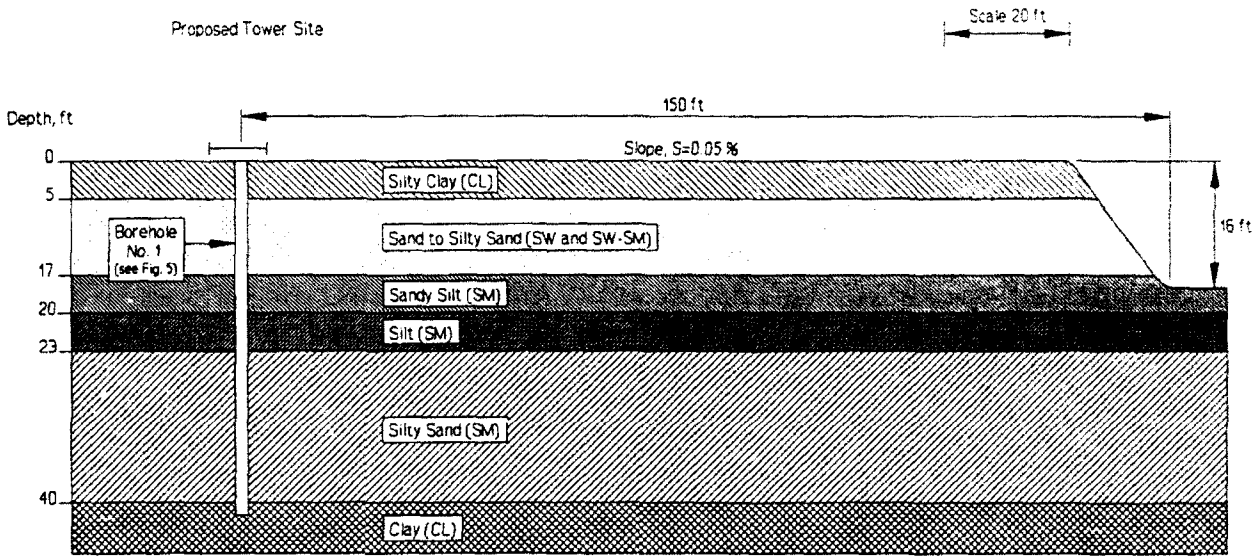

FIGURE 17

Hypothetical Cross Section of Site for Example Calculations

TABLE 1

Representative Number of Cycles and Magnitude Scaling Factors for Various Earthquake Magnitudes (After NRC, 1985)

Earthquake Magnitude (M)	Number of Representative Cycles at 0.65 τ_{max}	Factor to Correct Abscissa of Curve in Figure 4-3
8.5	26	0.89
7.5	15	1.0
6.75	10	1.13
6.0	5-6	1.32
5.25	2-3	1.5

SOURCE: After Seed and Idriss (1982).

TABLE 2

Summary of Energy Ratios for SPT Procedures (After NRC, 1985)

Country	Hammer Type	Hammer Release	Estimated Rod Energy (Percent)	Correction Factor for 60 Percent Rod Energy
Japan[a]	Donut	Free-fall	78	78/60 = 1.30
	Donut	Rope and pulley with special throw release	67	67/60 = 1.12
United States	Safety	Rope and pulley	60	60/60 = 1.00
	Donut[b]	Rope and pulley	45	45/60 = 0.75
Argentina	Donut	Rope and pulley	45	45/60 = 0.75
China	Donut	Free-fall[c]	60	60/60 = 1.00
	Donut	Rope and pulley	50	50/60 = 0.83

[a]Japanese SPT results have additional corrections for borehole diameter and frequency effects.
[b]Prevalent method in the United States today.
[c]Pilcon-type hammers develop an energy ratio of about 60 percent.
SOURCE: Seed et al. (1984).

TABLE 3

Data and Results for Calculations of Liquefaction Susceptibility For A Magnitude 6.5 Earthquake Generating an 0.30 g Peak Acceleration Shaking The Soil Profile Shown in Figure 5

Depth ft	Soil Description	N_m blow/ft	$(N_1)_{60}$ blow/ft	Fines %	Clay %	D_{50} mm	Unit Weight lb/ft^3	CSRL	CSRE	Factor of Safety
3	Silty clay (CL)	NA		87	43		110	NA	0.19	NA
6	Sand (SW)	6	8.5 ?	3	0	0.43	120	0.12	0.24	0.50
9	Sand (SW)	5	6.2 ?	5	0	0.51	120	0.07	0.27	0.26
12	Sand with silt (SW-SM)	15	18.6	10	0	0.31	120	0.30	0.29	1.02
15	Sand with silt (SW-SM)	12	13.6	8	0	0.37	120	0.20	0.31	0.63
18	Silty sand (SM)	9	9.4	43	2	0.11	120	0.21	0.32	0.66
21	Silt (ML)	9	8.8	88	13	0.03	120	NA	0.32	NA
24	Silty sand (SM)	17	15.9	21	0	0.22	120	0.30	0.33	0.92
27	Silty sand (SM)	18	15.9	30	1	0.20	120	0.33	0.33	1.00
30	Silty sand (SM)	21	17.7	37	1	0.18	120	0.47	0.33	1.42
33	Silty sand (SM)	31	25.1	35	0	0.25	120	>1	0.33	>2
36	Silty sand (SM)	33	25.6	28	0	0.23	120	>1	0.32	>2
39	Silty sand (SM)	32	24.0	18	0	0.30	120	>1	0.31	>2
42	Clay (ML)									

TABLE 4

Earthquakes and Lateral Spread Sites Included in Case-History Database
(After Bartlett and Youd, 1992)

1906 San Francisco Earthquake

Coyote Creek Bridge near Milpitas, California
Mission Creek Zone in San Francisco, California
Salinas River Bridge near Salinas, California
South of Market Street Zone in San Francisco, California

1964 Alaska Earthquake

Bridges 141.1, 147.4, 147.5, 148.3, Matanuska River, Alaska
Bridges 63.0, 63.5, Portage Creek, Portage, Alaska
Highway Bridge 629, Placer River, Alaska (Ross et al., 1973)
Snow River Bridge 605A, Snow River, Alaska (Ross et al., 1973)
Bridges 3.0, 3.2, 3.3, Resurrection River, Alaska

1964 Niigata, Japan, Earthquake

Numerous lateral spreads in Niigata, Japan

1971 San Fernando, California Earthquake

Jensen Filtration Plant
Juvenile Hall

1979 Imperial Valley, California Earthquake

Heber Road near El Centro, California
River Park near Brawley, California

1983 Borah Peak Idaho, Earthquake

Whiskey Springs near Mackay, Idaho
Pence Ranch near Mackay, Idaho

1983 Nihonkai-Chubu Earthquake

Lateral spreads in the Northern Sector of Noshiro, Japan

1987 Superstition Hills Earthquake

Wildlife Instrument Array, Brawley, CA

TABLE 5

Ranges of Input Values for Independent Variables for Which Predicted Results Are Verified by Case-History Observations (After Bartlett and Youd, 1992)

Input Factor	Range of Values in Case History Database
Magnitude	$6.0 < M < 8.0$
Free-Face Ratio	$1.0\% < W < 20\%$
Ground Slope	$0.1\% < S < 6\%$
Thickness of Loose Layer	$0.3\ m < T_{15} < 12\ m$
Fines Content	$0\% < F_{15} < 50\%$
Mean Grain Size	$0.1\ mm < D50_{15} < 1\ mm$
Depth to Bottom of Section	Depth to Bottom of Liquefied Zone < 15 m

TABLE 6

Minimum Values of R That Should Be Applied in Equation 5 (After Bartlett and Youd, 1992)

M	R (km)	M	R (km)	M	R (km)
6.5	0.25	7.4	2.4	8.3	17
6.6	0.3	7.5	3	8.4	20
6.7	0.4	7.6	4	8.5	24
6.8	0.5	7.7	5	8.6	28
6.9	0.7	7.8	6	8.7	33
7.0	0.9	7.9	8	8.8	38
7.1	1.1	8.0	9	8.9	43
7.2	1.4	8.1	12	9.0	50
7.3	1.8	8.2	14		

DISTRIBUTION LIST

1SG/CEEE / LT MARSH, LANGLEY AFB, VA
AF / 438 ABG/DEE (WILSON), MCGUIRE AFB, NJ
AFB / HQ TAC/DEMM (POLLARD), LANGLEY AFB, VA
AFESC / TECH LIB, TYNDALL AFB, FL
AMERICAN CONCRETE / LIB, DETROIT, MI
ARMY / CEHSC-FU-N (KRAJEWSKI), FORT BELVOIR, VA; R&D LAB, STRNC-UE, NATICK, MA
ARMY CECOM R&D TECH LIBRARY / ASNC-ELC-I-T, FORT MONMOUTH, NJ
ARMY CERL / CECER-FME (HAYES), CHAMPAIGN, IL; LIB, CHAMPAIGN, IL
ARMY DEPOT / LETTERKENNY, SDSLE-EN, CHAMBERSBURG, PA
ARMY ENGRG DIST / CENPS-ED-SD, SEATTLE, WA; LIB, PHILADELPHIA, PA; LIB, SEATTLE, WA
ARMY ENGRG DIV / CEEUD-ED-TA (MCVAY), FRANKFURT, GE, APO AE; CEHND-ED-CS, HUNTSVILLE, AL; ED-SY (LOYD), HUNTSVILLE, AL
ARMY EWES / CEWES-CD-P, VICKSBURG, MS; LIB, VICKSBURG, MS; WESCD-P (MELBY), VICKSBURG, MS
ARMY MISSILE R&D CMD / CH, DOCS, SCI INFO CTR, REDSTONE ARSENAL, AL
ARVID GRANT & ASSOC / OLYMPIA, WA
ASO / PWO, PHILADELPHIA, PA; PWP-A, PHILADELPHIA, PA
ATLANTIC RICHFIELD CO / RE SMITH, DALLAS, TX
BATTELLE / D. FRINK, COLUMBUS, OH
BECHTEL CIVIL, INC / K. MARK, SAN FRANCISCO, CA
BEN C GERWICK INC / FOTINOS, SAN FRANCISCO, CA
BETHLEHEM STEEL CO / ENGRG DEPT, BETHLEHEM, PA
BLAYLOCK ENGINEERING GROUP / T SPENCER, SAN DIEGO, CA
BRITISH EMBASSY / SCI & TECH DEPT (WILKINS), WASHINGTON, DC
BROWN, ROBERT / TUSCALOOSA, AL
BULLOCK, TE / LA CANADA, CA
BUREAU OF RECLAMATION / D-1512 (GS DEPUY), DENVER, CO
CAL STATE UNIV / C.V. CHELAPATI, LONG BEACH, CA
CASE WESTERN RESERVE UNIV / CE DEPT (PERDIKARIS), CLEVELAND, OH
CBC / CODE 430, GULFPORT, MS; PWO (CODE 400), GULFPORT, MS
CESO / CODE 155, PORT HUENEME, CA
CHAO, JC / HOUSTON, TX
CHEE, WINSTON / GRETNA, LA
CHESNAVFACENGCOM / CODE 112.1, WASHINGTON, DC; CODE 402 (FRANCIS), WASHINGTON, DC; CODE 407, WASHINGTON, DC; YACHNIS, WASHINGTON, DC
CHEVRON OIL FLD RSCH CO / ALLENDER, LA HABRA, CA
CHILDS ENGRG CORP / K.M. CHILDS, JR., MEDFIELD, MA
CITY OF SACRAMENTO / GEN SVCS DEPT, SACRAMENTO, CA
CITY OF WINSTON-SALEM / RJ ROGERS, PWD, WINSTON SALEM, NC
CLARK, T. / SAN MATEO, CA
CLARKSON UNIV / CEE DEPT, POTSDAM, NY
COGUARD / SUPERINTENDENT, NEW LONDON, CT
COLLEGE OF ENGINEERING / CE DEPT (GRACE), SOUTHFIELD, MI
COLLINS ENGRG, INC / M GARLICH, CHICAGO, IL
COLORADO STATE UNIV / CE DEPT (CRISWELL), FORT COLLINS, CO
COMCBLANT / CODE S3T, NORFOLK, VA
COMFLEACT / PWO, FPO AP

COMNAVSURF / CODE N42A, NORFOLK, VA
CONRAD ASSOC / LUISONI, VAN NUYS, CA
CONSOER TOWNSEND & ASSOC / DEBIAK, CHICAGO, IL
CONSTRUCTION TECH LABS, INC / G. CORLEY, SKOKIE, IL
CORNELL UNIV / CIVIL & ENVIRON ENGRG, ITHACA, NY; LIB, ITHACA, NY
DAMES & MOORE / LIB, LOS ANGELES, CA
DAVY DRAVO / WRIGHT, PITTSBURG, PA
DELAWARE / EMERGENCY MGMT, DELAWARE CITY, DE
DEPT OF BOATING / ARMSTRONG, SACRAMENTO, CA
DEPT OF STATE / FOREIGN BLDGS OPS, BDE-ESB, ARLINGTON, VA
DFSC-F / ALEXANDRIA, VA
DOBROWOLSKI, JA / ALTADENA, CA
DOD / EXPLOS SAFETY BRD, ALEXANDRIA, VA
DTRCEN / CODE 172, BETHESDA, MD
EDWARD K NODA & ASSOC / HONOLULU, HI
ENGINEERING DATA MANAGEMENT / RONALD W. ANTHONY, FORT COLLINS, CO
ESCO SCIENTIFIC PRODUCTS (ASIA) / PTE LTD, CHAI
FAA / ARD 200, WASHINGTON, DC
FACILITIES DEPT / FACILITIES OFFICER, FPO AP
FLORIDA ATLANTIC UNIV / OCEAN ENGRG DEPT (MARTIN), BOCA RATON, FL; OCEAN ENGRG DEPT (SU), BOCA RATON, FL
GEI CONSULTANTS, INC. / T.C. DUNN, WINCHESTER, MA
GEIGER ENGINEERS / FUNSTON, BELLINGHAM, WA
GEOCON INC / CORLEY, SAN DIEGO, CA
GEORGE WASHINGTON UNIV / ENGRG & APP SCI SCHL (FOX), WASHINGTON, DC
GEORGIA INST OF TECH / CE SCHL (KAHN), ATLANTA, GA; CE SCHL (SWANGER), ATLANTA, GA; CE SCHL (ZURUCK), ATLANTA, GA
GERWICK, BEN / SAN FRANCISCO, CA
GIORDANO, A.J. / SEWELL, NJ
GRUMMAN AEROSPACE CORP / TECH INFO CENTER, BETHPAGE, NY
GSA / HALL, WASHINGTON, DC
HAN-PADRON ASSOCIATES / DENNIS PADRON, NEW YORK, NY
HARDY, S.P. / SAN RAMON, CA
HARTFORD STEAM BOILER INSP & INS CO / SPINELLI, HARTFORD, CT
HAYNES & ASSOC / H. HAYNES, PE, OAKLAND, CA
HAYNES, B / LYNDEN, WA
HEUZE, F / ALAMO, CA
HJ DEGENKOLB ASSOC / W. MURDOUGH, SAN FRANCISCO, CA
HOIDRA / NEW YORK, NY
HOPE ARCHTS & ENGRS / SAN DIEGO, CA
HQ AFLC / CAPT SCHMIDT, WRIGHT PATTERSON AFB, OH
HUGHES AIRCRAFT CO / TECH DOC CEN, EL SEGUNDO, CA
INFOTEAM INC / M. ALLEN, PLANTATION, FL
INST OF MARINE SCIENCES / LIB, PORT ARANSAS, TX
INTL MARITIME, INC / D. WALSH, SAN PEDRO, CA
JOHN HOPKINS UNIV / CE DEPT, JONES, BALTIMORE, MD
JOHN J MC MULLEN ASSOC / LIB, NEW YORK, NY
KAISER PERMANENTE MEDCIAL CARE PROGRAM / OAKLAND, CA
LAWRENCE LIVERMORE NATL LAB / FJ TOKARZ, LIVERMORE, CA; PLANT ENGRG LIB (L-654), LIVERMORE, CA
LEO A DALY CO / HONOLULU, HI
LIN OFFSHORE ENGRG / P. CHOW, SAN FRANCISCO, CA

LONG BEACH PORT / ENGRG DIR (ALLEN), LONG BEACH, CA; ENGRG DIR (LUZZI), LONG BEACH, CA
MARATHON OIL CO / GAMBLE, HOUSTON, TX
MARCORBASE / CODE 4.01, CAMP PENDLETON, CA; CODE 406, CAMP LEJEUNE, NC; FACILITIES COORDINATOR, CAMP PENDLETON, CA; PAC, PWO, FPO AP
MARITECH ENGRG / DONOGHUE, AUSTIN, TX
MCAS / CODE 1JE.50 (ISAACS), SANTA ANA, CA; CODE LE, CHERRY POINT, NC
MCRD / PWO, SAN DIEGO, CA
MICHIGAN TECH UNIV / CO DEPT (HAAS), HOUGHTON, MI
MOBIL R&D CORP / OFFSHORE ENGRG LIB, DALLAS, TX
MT DAVISSON / CE, SAVOY, IL
NAF / ENGRG DIV, PWD, FPO AP; PWO, FPO AP
NAS / CODE 18300, LEMOORE, CA; CODE 421, SAN DIEGO, CA; CODE 8, PATUXENT RIVER, MD; CODE 85GC, GLENVIEW, IL; DIR, ENGRG DIV, PWD, KEFLAVIK, ICELAND, FPO AE; FAC MGMT OFFC, ALAMEDA, CA; MIRAMAR, SAN DIEGO, CA; MIRAMAR, PWO, SAN DIEGO, CA; PWO, KEY WEST, FL; PWO, CECIL FIELD, FL; PWO, SIGONELLA, ITALY, FPO AE; SCE, BARBERS POINT, HI; WHITING FLD, PWO, MILTON, FL
NAS OCEANA / ADAMETZ, VIRGINIA BEACH, VA
NAVAIRDEVCEN / CODE 832, WARMINSTER, PA
NAVAVNDEPOT / CODE 640, PENSACOLA, FL
NAVCOASTSYSCEN / PWO (CODE 740), PANAMA CITY, FL
NAVCOMMSTA / PWO, FPO AP
NAVEODTECHCEN / TECH LIB, INDIAN HEAD, MD
NAVFAC / PWO (CODE 50), BRAWDY WALES, UK, FPO AE; PWO, OAK HARBOR, WA
NAVFACENGCOM / CODE 04A3, ALEXANDRIA, VA; CODE 07, ALEXANDRIA, VA; CODE 07M (BENDER), ALEXANDRIA, VA
NAVMAG / SCE, FPO AP
NAVMEDCOM / NWREG, FAC ENGR, PWD, OAKLAND, CA
NAVOCEANO / CODE 6200 (M PAIGE), NSTL, MS
NAVPGSCOL / PWO, MONTEREY, CA
NAVPHIBASE / PWO, NORFOLK, VA; SCE, SAN DIEGO, CA
NAVSCOLCECOFF / CODE C35, PORT HUENEME, CA
NAVSCSCOL / PWO, ATHENS, GA
NAVSECGRUACT / CODE 31 PWO, FPO AA
NAVSHIPREFAC / LIB, FPO AP; SCE, FPO AP
NAVSHIPYD / CODE 244.13, LONG BEACH, CA; CODE 440, PORTSMOUTH, VA; MARE IS, PWO, VALLEJO, CA; TECH LIB, PORTSMOUTH, NH
NAVSTA / CODE N4214, MAYPORT, FL; ENGR DIV, PWD, FPO AA; ENGRG DIR, PWD, ROTA, SPAIN, FPO AE
NAVSTA PANAMA CANAL / CODE 54, FPO AA
NAVSUPACT / CODE 430, NEW ORLEANS, LA; PWO, NAPLES, ITALY, FPO AE
NAVSUPSYSCOM / CODE 0622, WASHINGTON, DC
NAVSWC / CODE W41C1, DAHLGREN, VA
NAVWPNCEN / PWO (CODE 266), CHINA LAKE, CA
NAVWPNSTA / CODE 092B (HUNT), YORKTOWN, VA; CODE 104, CHARLESTON, SC; PWO, YORKTOWN, VA
NCCOSC / CODE 9642, SAN DIEGO, CA
NEESA / CODE 111E (MCCLAINE), PORT HUENEME, CA
NEW MEXICO SOLAR ENERGY INST / LAS CRUCES, NM
NEW ZEALAND CONCRETE RSCH ASSN / LIB, PORIRUA,
NIEDORODA, AW / GAINESVILLE, FL

NOAA / JOSEPH VADUS, ROCKVILLE, MD
NORTHNAVFACENGCOM / CO, PHILADELPHIA, PA
NRL / CODE 4670, WASHINGTON, DC
NSY / CODE 214.3 (WEBER), PORTSMOUTH, VA
NUHN & ASSOC / A.C. NUHN, WAYZATA, NM
NUSC DET / CODE 2143 (VARLEY), NEW LONDON, CT; CODE 44 (MUNN), NEW LONDON, CT; CODE TA131, NEW LONDON, CT; LIB, NEWPORT, RI; PWO, NEW LONDON, CT
OICC / ENGR AND CONST DEPT, APO AE
OMEGA MARINE, INC. / SCHULZE, LIBRARIAN, HOUSTON, TX
OREGON STATE UNIV / CE DEPT (HICKS), CORVALLIS, OR
PACIFIC MARINE TECH / M. WAGNER, DUVALL, WA
PACNAVFACENGCOM / CODE 102, PEARL HARBOR, HI
PENNSYLVANIA STATE UNIV / GOTOLSKI, UNIVERSITY PARK, PA; RSCH LAB, STATE COLLEGE, PA
PERKOWSKI, MICHAEL T. / TIPPECANOE, OH
PILE BUCK, INC / SMOOT, JUPITER, FL
PMB ENGRG / LUNDBERG, SAN FRANCISCO, CA
PMTC / CODE 1018, POINT MUGU, CA; CODE 5041, POINT MUGU, CA; CODE P4234 (G. NUSSEAR), POINT MUGU, CA
PORTLAND CEMENT ASSOC / AE FIORATO, SKOKIE, IL
PORTLAND STATE UNIV / ENGRG DEPT (MIGLIORI), PORTLAND, OR
PURDUE UNIV / CE SCOL (CHEN), WEST LAFAYETTE, IN; CE SCOL (LEONARDS), WEST LAFAYETTE, IN
PWC / CODE 102, OAKLAND, CA; CODE 123C, SAN DIEGO, CA; CODE 400, OAKLAND, CA; CODE 400A.3, FPO AP; CODE 420, OAKLAND, CA; CODE 421 (KAYA), PEARL HARBOR, HI; CODE 421 (REYNOLDS), SAN DIEGO, CA; CODE 421, NORFOLK, VA; CODE 422, SAN DIEGO, CA; CODE 423, SAN DIEGO, CA
SAN DIEGO PORT / PORT FAC, PROJ ENGR, SAN DIEGO, CA
SAN DIEGO STATE UNIV / CE DEPT (KRISHNAMOORTHY), SAN DIEGO, CA
SANDIA LABS / LIB, LIVERMORE, CA
SARGENT & HERKES, INC / JP PIERCE, JR, NEW ORLEANS, LA
SEATECH CORP / PERONI, MIAMI, FL
SEATTLE PORT / DAVE VAN VLEET, SEATTLE, WA; DAVID TORSETH, SEATTLE, WA
SEATTLE UNIV / CE DEPT (SCHWAEGLER), SEATTLE, WA
SHELL OIL CO / E. DOYLE, HOUSTON, TX
SIMPSON, GUMPERTZ & HEGER, INC / HILL, ARLINGTON, MA
SMELSER, D / SEVIERVILLE, TN
SOUTHNAVFACENGCOM / CODE 04A, CHARLESTON, SC; CODE 102H, CHARLESTON, SC; CODE 1622, CHARLESTON, SC
SOUTHWEST RSCH INST / ENERGETIC SYS DEPT (ESPARZA), SAN ANTONIO, TX; KING, SAN ANTONIO, TX; M. POLCYN, SAN ANTONIO, TX; MARCHAND, SAN ANTONIO, TX; THACKER, SAN ANTONIO, TX
SOWESTNAVFACENGCOM / LANGSTRAAT, SAN DIEGO, CA
SPCC / PWO, MECHANICSBURG, PA
STATE UNIV OF NEW YORK / CE DEPT, BUFFALO, NY
SUPSHIP / TECH LIB, NEWPORT, VA
TEXAS A&M UNIV / CE DEPT (MACHEMEHL), COLLEGE STATION, TX; CE DEPT (NIEDZWECKI), COLLEGE STATION, TX; OCEAN ENGR PROJ, COLLEGE STATION, TX
THE WORLD BANK / ARMSTRONG, WASHINGTON, DC
TRW INC / ENGR LIB, CLEVELAND, OH
TRW SPACE AND TECHNOLOGY GROUP / CARPENTER, REDONDO BEACH, CA

TUDOR ENGRG CO / ELLEGOOD, PHOENIX, AZ
UNIV OF CALIFORNIA / CE DEPT (FENVES), BERKELEY, CA; CE DEPT (FOURNEY), LOS ANGELES, CA; CE DEPT (TAYLOR), DAVIS, CA; CE DEPT (WILLIAMSON), BERKELEY, CA; NAVAL ARCHT DEPT, BERKELEY, CA
UNIV OF HAWAII / CE DEPT (CHIU), HONOLULU, HI; MANOA, LIB, HONOLULU, HI; OCEAN ENGRG DEPT (ERTEKIN), HONOLULU, HI; RIGGS, HONOLULU, HI
UNIV OF ILLINOIS / METZ REF RM, URBANA, IL
UNIV OF MARYLAND / CE DEPT, COLLEGE PARK, MD
UNIV OF MICHIGAN / CE DEPT (RICHART), ANN ARBOR, MI
UNIV OF N CAROLINA / CE DEPT (AHMAD), RALEIGH, NC
UNIV OF NEW MEXICO / NMERI (BEAN), ALBUQUERQUE, NM; NMERI, HL SCHREYER, ALBUQUERQUE, NM
UNIV OF PENNSYLVANIA / DEPT OF ARCH, PHILADELPHIA, PA
UNIV OF RHODE ISLAND / CE DEPT (KARAMANLIDIS), KINGSTON, RI; CE DEPT (KOVACS), KINGSTON, RI; CE DEPT (TSIATAS), KINGSTON, RI; DR. VEYERA, KINGSTON, RI
UNIV OF TEXAS / CONSTRUCTION INDUSTRY INST, AUSTIN, TX; ECJ 4.8 (BREEN), AUSTIN, TX
UNIV OF WASHINGTON / CE DEPT (HARTZ), SEATTLE, WA; CE DEPT (MATTOCK), SEATTLE, WA
UNIV OF WISCONSIN / GREAT LAKES STUDIES CEN, MILWAUKEE, WI
UNIV OF WYOMING / SCHMIDT, LARAMIE, WY
US NUCLEAR REGULATORY COMMISSION / KIM, WASHINGTON, DC
USACOE / CESPD-CO-EQ, SAN FRANCISCO, CA
USAE / CEWES-IM-MI-R, VICKSBURG, MS
USDA / FOR SVC, REG BRIDGE ENGR, ALOHA, OR
USNA / CH, MECH ENGRG DEPT (C WU), ANNAPOLIS, MD; OCEAN ENGRG DEPT, ANNAPOLIS, MD; PWO, ANNAPOLIS, MD
USPS / BILL POWELL, WASHINGTON, DC
VALLEY FORGE CORPORATE CENTER / FRANKLIN RESEARCH CENTER, NORRISTOWN, PA
VAN ALLEN, B / KINGSTON, NY
VSE / OCEAN ENGRG GROUP (MURTON), ALEXANDRIA, VA
VSE CORP / LOWER, ALEXANDRIA, VA
VULCAN IRON WORKS, INC / DC WARRINGTON, CLEVELAND, TN
WESTINGHOUSE ELECTRIC CORP / LIB, PITTSBURG, PA
WESTNAVFACENGCOM / VALDEMORO, SAN BRUNO, CA
WISS, JANNEY, ELSTNER, & ASSOC / DW PFEIFER, NORTHBROOK, IL
WISWELL, INC. / SOUTHPORT, CT
WOODWARD-CLYDE CONSULTANTS / WEST REG, LIB, OAKLAND, CA

DISTRIBUTION QUESTIONNAIRE

The Naval Civil Engineering Laboratory is revising its primary distribution lists.

SUBJECT CATEGORIES

1 **SHORE FACILITIES**
1A Construction methods and materials (including corrosion control, coatings)
1B Waterfront structures (maintenance/deterioration control)
1C Utilities (including power conditioning)
1D Explosives safety
1E Aviation Engineering Test Facilities
1F Fire prevention and control
1G Antenna technology
1H Structural analysis and design (including numerical and computer techniques)
1J Protective construction (including hardened shelters, shock and vibration studies)
1K Soil/rock mechanics
1L Airfields and pavements
1M Physical security
2 **ADVANCED BASE AND AMPHIBIOUS FACILITIES**
2A Base facilities (including shelters, power generation, water supplies)
2B Expedient roads/airfields/bridges
2C Over-the-beach operations (including breakwaters, wave forces)
2D POL storage, transfer, and distribution
2E Polar engineering
3 **ENERGY/POWER GENERATION**
3A Thermal conservation (thermal engineering of buildings, HVAC systems, energy loss measurement, power generation)
3B Controls and electrical conservation (electrical systems, energy monitoring and control systems)
3C Fuel flexibility (liquid fuels, coal utilization, energy from solid waste)
3D Alternate energy source (geothermal power, photovoltaic power systems, solar systems, wind systems, energy storage systems)
3E Site data and systems integration (energy resource data, integrating energy systems)
3F EMCS design
4 **ENVIRONMENTAL PROTECTION**
4A Solid waste management
4B Hazardous/toxic materials management
4C Waterwaste management and sanitary engineering
4D Oil pollution removal and recovery
4E Air pollution
4F Noise abatement
5 **OCEAN ENGINEERING**
5A Seafloor soils and foundations
5B Seafloor construction systems and operations (including diver and manipulator tools)
5C Undersea structures and materials
5D Anchors and moorings
5E Undersea power systems, electromechanical cables, and connectors
5F Pressure vessel facilities
5G Physical environment (including site surveying)
5H Ocean-based concrete structures
5J Hyperbaric chambers
5K Undersea cable dynamics
ARMY FEAP
BDG Shore Facilities
NRG Energy
ENV Environmental/Natural Responses
MGT Management
PRR Pavements/Railroads

TYPES OF DOCUMENTS

D - Techdata Sheets; **R** - Technical Reports and Technical Notes; **G** - NCEL Guides and Abstracts; **I** - Index to TDS; **U** - User Guides; ☐ None - remove my name

Old Address:

_____

_____

_____

_____

Telephone No.: _____

New Address:

_____

_____

_____

_____

Telephone No.: _____

INSTRUCTIONS

The Naval Civil Engineering Laboratory has revised its primary distribution lists. To help us verify our records and update our data base, please do the following:

- Add - circle number on list
- Remove my name from all your lists - check box on list.
- Change my address - line out incorrect line and write in correction **(DO NOT REMOVE LABEL).**
- Number of copies should be entered after the title of the subject categories you select.
- Are we sending you the correct type of document? If not, circle the type(s) of document(s) you want to receive listed on the back of this card.

Fold on line, staple, and drop in mail.

DEPARTMENT OF THE NAVY
Naval Civil Engineering Laboratory
560 Laboratory Drive
Port Hueneme CA 93043-4328

Official Business
Penalty for Private Use, $300

NO POSTAGE NECESSARY IF MAILED IN THE UNITED STATES

BUSINESS REPLY CARD

FIRST CLASS PERMIT NO. 12503 WASH D.C.

POSTAGE WILL BE PAID BY ADDRESSEE

COMMANDING OFFICER
CODE L34
560 LABORATORY DRIVE
NAVAL CIVIL ENGINEERING LABORATORY
PORT HUENEME CA 93043-4328

NCEL DOCUMENT EVALUATION

You are number one with us; how do we rate with you?

We at NCEL want to provide you our customer the best possible reports but we need your help. Therefore, I ask you to please take the time from your busy schedule to fill out this questionnaire. Your response will assist us in providing the best reports possible for our users. I wish to thank you in advance for your assistance. I assure you that the information you provide will help us to be more responsive to your future needs.

R. N. STORER, Ph.D, P.E.
Technical Director

DOCUMENT NO. _____ TITLE OF DOCUMENT: _____

_____

Date: _____ Respondent Organization : _____

Name: _____ Activity Code: _____
Phone: _____ Grade/Rank: _____

Category (*please check*):

Sponsor ____ User ____ Proponent ____ Other (*Specify*) _____

Please answer on your behalf only; not on your organization's. Please check (*use an X*) only the block that most closely describes your attitude or feeling toward that statement:

SA Strongly Agree A Agree O Neutral D Disagree SD Strongly Disagree

---

	SA	A	N	D	SD
1. The technical quality of the report is comparable to most of my other sources of technical information.	( )	( )	( )	( )	( )
2. The report will make significant improvements in the cost and or performance of my operation.	( )	( )	( )	( )	( )
3. The report acknowledges related work accomplished by others.	( )	( )	( )	( )	( )
4. The report is well formatted.	( )	( )	( )	( )	( )
5. The report is clearly written.	( )	( )	( )	( )	( )
6. The conclusions and recommendations are clear and directly supported by the contents of the report.	( )	( )	( )	( )	( )
7. The graphics, tables, and photographs are well done.	( )	( )	( )	( )	( )

Do you wish to continue getting NCEL reports? ☐ YES ☐ NO

Please add any comments (e.g., in what ways can we improve the quality of our reports?) on the back of this form.

Comments:

Fold on line, staple, and drop in mail.

DEPARTMENT OF THE NAVY
Naval Civil Engineering Laboratory
560 Laboratory Drive
Port Hueneme CA 93043-4328

Official Business
Penalty for Private Use, $300

NO POSTAGE NECESSARY IF MAILED IN THE UNITED STATES

BUSINESS REPLY CARD

FIRST CLASS PERMIT NO. 12503 WASH D.C.

POSTAGE WILL BE PAID BY ADDRESSEE

COMMANDING OFFICER
CODE L03
560 LABORATORY DRIVE
NAVAL CIVIL ENGINEERING LABORATORY
PORT HUENEME CA 93043-4328